



THE UNIVERSITY OF
WAIKATO
Te Whare Wānanga o Waikato

Research Commons

<http://waikato.researchgateway.ac.nz/>

Research Commons at the University of Waikato

Copyright Statement:

The digital copy of this thesis is protected by the Copyright Act 1994 (New Zealand).

The thesis may be consulted by you, provided you comply with the provisions of the Act and the following conditions of use:

- Any use you make of these documents or images must be for research or private study purposes only, and you may not make them available to any other person.
- Authors control the copyright of their thesis. You will recognise the author's right to be identified as the author of the thesis, and due acknowledgement will be made to the author where appropriate.
- You will obtain the author's permission before publishing any material from the thesis.

CHAPTER ONE - Introduction

1.0 Introduction

The Gisborne Region covers a land area of 8,265 km₂ on the east coast of the North Island of New Zealand. This is approximately 4.9% of New Zealand's total land area. Neighboring regions are Hawkes Bay to the south and the Bay of Plenty to the north west (Figure 1).

Provisional data from the 2006 census indicate that the population of the main city of Gisborne is ~44,400. The other major population centers are Ruatoria (~720), Tokomaru Bay (~450), Tolaga Bay (~860), and Te Karaka (~530) (Statistics New Zealand 2005).



Figure 1 Image of the East Cape on the North Island, showing Gisborne, Tolaga Bay, Tokomaru Bay

Chapter One – Introduction

The local authorities (Civil Defense) in Gisborne are aware of the risk and threat that tsunami pose to the region (Friday the 11th of May 2007 was the 130-year anniversary of a major tsunami that struck the area following an 8.3 magnitude earthquake off the coast of South America, also the recent earthquake in December 2007 was a reminder about Gisborne vulnerability.

The East Coast has experienced >15 tsunami events since 1868. Distant tsunamis have originated from South America (3), Indonesia (2), Kamchatka and Alaska (2), and Tonga (2-3). The largest rise in sea level recorded from any of the distantly generated events has been between 2 and 4 m above normal high tide. The Pacific Warning Centre in Hawaii would provide sufficient warning for one of these events to effect an orderly evacuation.

The Gisborne district has experienced at least 4 locally generated tsunami since 1868; the largest had heights >10 m, and the second largest was around 5-6 m. These were generated around the Ariel Bank in 1947 approximately 15 km off the coast. A small earthquake preceded both of them with the waves impacting between 15 and 30 minutes later. There is the possibility that the size of the wave was increased by a mud volcanic eruption or undersea landslide. This raises the potential for a wave to be generated with no earthquake at all. Two other smaller events have been recorded in Tolaga Bay in 1926 and 1970.

The whole Gisborne District coastline is at risk from a locally generated tsunami. The risk to Gisborne city is significant. Apart from known tsunami sources the recent discovery of canyons capable of producing undersea landslides of 1500 km³, starting approximately 15 km outside of Poverty Bay, also adds to the threat of tsunami. The presence of mud volcanic activity inside the Bay also enhances the risk.

Chapter One – Introduction

A recent appraisal of tsunami threat (Berryman 2004) indicated that Gisborne could have over 500 fatalities as a result of in a 1 in 2500 year likelihood tsunami event, assuming zero warning system effectiveness. While Gisborne can reduce the level of multiple fatalities with effective distant-source warning systems, there is still a significant outstanding risk from local sources, which will require mitigation through a range of measures.

1.2 Thesis Aims and Objectives

The aim of this thesis is to determine the likely extent of tsunami inundation for Gisborne City and surrounding populated coastal locations in Poverty Bay.

Determine the likely extent of tsunami inundation for Gisborne City and surrounding populated coastal locations in Poverty Bay, using a combination of hydrodynamic tsunami modeling and GIS. The modeling will be based on a historical event, particularly the largest historical tsunami, May 1947 local tsunami generated by a submarine landslide.

Modeling will also consider potential events based on the Maximum Credible Earthquake for local sources associated with the Hikurangi Deformation Front.

Specific objectives to achieve this are:

- Define the Maximum Credible Tsunami (MCT) by evaluating historical tsunami events and seismicity for the region. This will define the initial conditions for the tsunami generation.
- Simulate the development and propagation of the MCT, and hence the subsequent inundation.
- Identify areas that are susceptible to tsunami inundation and determine what the likely impact will be and the extent of the damage.
- Create a hazard map that can be used for future town planning.

1.3 Study Area

This study focuses on the Poverty Bay coastline, extending from Young Nicks Head to Wainui (Figure 2). Gisborne City lies at the northern end of Poverty Bay, which faces South America, where large tsunamis capable of reaching New Zealand are generated on average every 45 years.

The other and much larger threat is that of a locally generated event. Large submarine canyons have been discovered offshore from Poverty Bay. Coupled with the high level of seismic activity and possessing one of the rivers with some of the highest sediment loads in the world creates the very real problem of submarine landslides.

Bathymetric surveys have been done of the bay and were used to help determine accurate water depths, for depths further out in the bay these were taken from LINZ map NZ5613 a map of Poverty Bay and approaches to Gisborne. Laser Imaging Detection and Ranging (system) (LiDAR) data has been used to accurately map the land heights.

Study Area - Poverty Bay

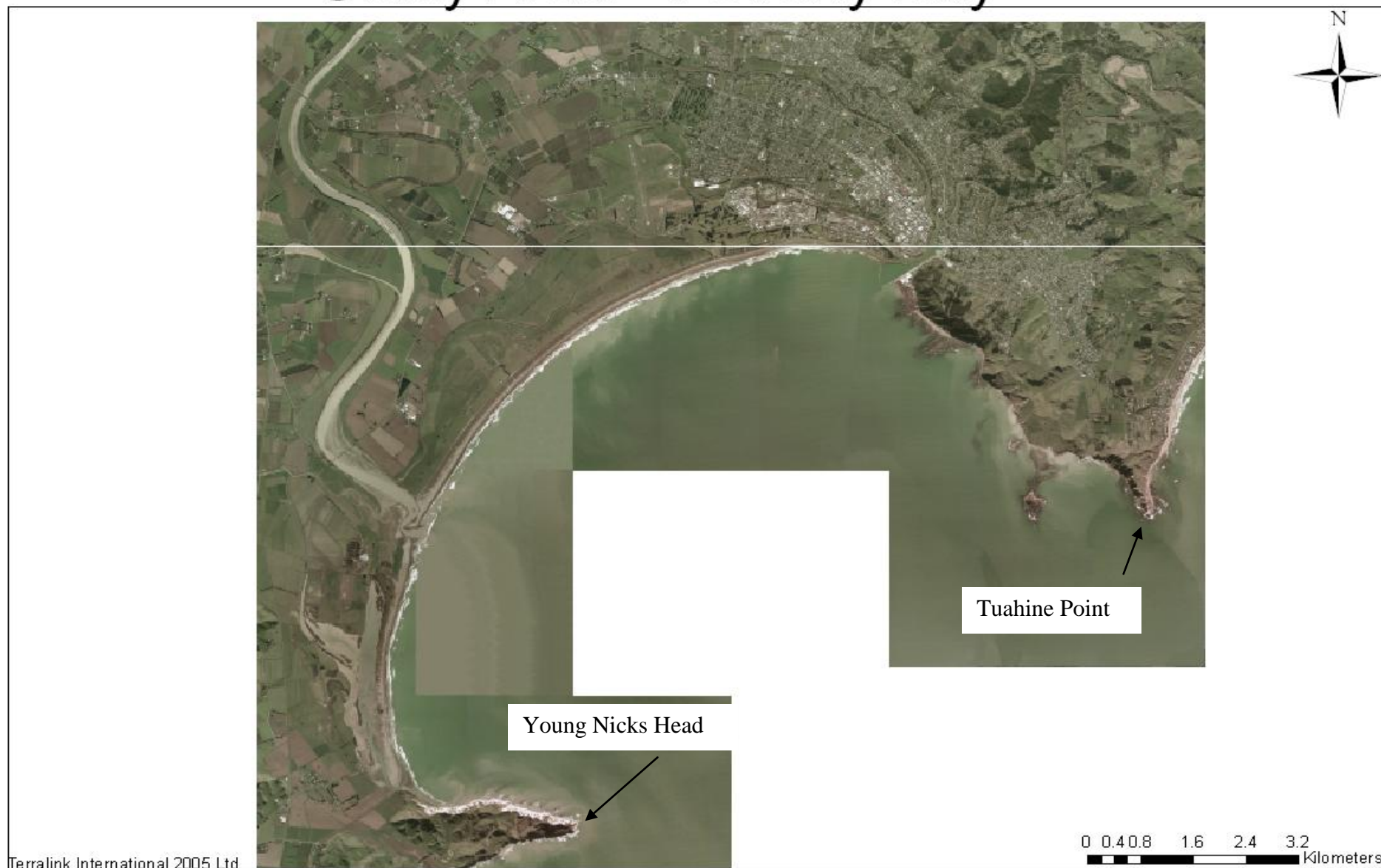


Figure 2 Aerial Photo of Gisborne coastline from Young Nicks Head to Wainui

Chapter One – Introduction

The local community is aware of the risk that a tsunami presents. In a recent poll undertaken by the Gisborne Herald 85% of the Gisborne people that voted said that something needed to be done about a warning system to help protect the local community. This is especially true with people fleeing up hills when they heard of a tsunami on the news and also more recently when local people once again took to the hills after the 2007 December 20th earthquake.

However, they do not fully comprehend the seriousness and magnitude of a locally generated event. The town at present is set up in a manner that has potential for greater problems than necessary i.e. the location of St Johns emergency services and the local Fire Brigade within areas that will be potentially inundated.

1.4 Research Outline

This thesis considers the current literature that deals with tsunamis and their affect on Gisborne. Chapter three looks in depth at Fault mechanisms and earthquakes affecting Gisborne.

Chapter four discusses the 3DD hydrodynamic model that has been used to create the models and looks at the methodology behind the model outputs.

Chapter five deals with the creation of the models, from start to finish.

Chapters 6 and 7 deals with the results and conclusions that resulted from the modeling.

CHAPTER TWO – Literature Review

2.0 What is a Tsunami?

There is widespread misunderstanding of what constitutes a tsunami. Although the popular notion of a tsunami is that of a large, breaking wave such as depicted as in the classical Hokusai picture of surf (not a tsunami) as he never saw one. A tsunami is any sudden, non-meteorologically-induced impulse in water regardless of size (Lander et al 2003).

Tsunami are a series of traveling ocean waves of extremely long length generated by earthquakes occurring below or near the ocean floor (Fig 1). Underwater volcanic eruptions and landslides can also generate tsunamis. In the deep ocean, the tsunami waves propagate across the deep ocean floor with a speed exceeding 800 kilometers per hour (km) and a wave height of only a few tens of centimeters or less. Tsunami waves are distinguished from ordinary ocean waves by their great length between wave crests, often exceeding a 100 km or more in the deep ocean, and by the time between the crests, ranging from 10 minutes to one hour (Karling 2005).

Tsunamis are waves that propagate away from an area where the sea surface has been subjected to a short-duration disturbance. They are usually generated by sub-sea earthquakes and rapidly radiate outwards from the area of initial disturbance. The Pacific Ocean with its seismically active margins, has many tsunamis. Locally generated tsunamis appear to produce short-period waves locally whereas distantly generated tsunamis appear to produce longer-period harbour and continental shelf oscillations (Heath 1985).

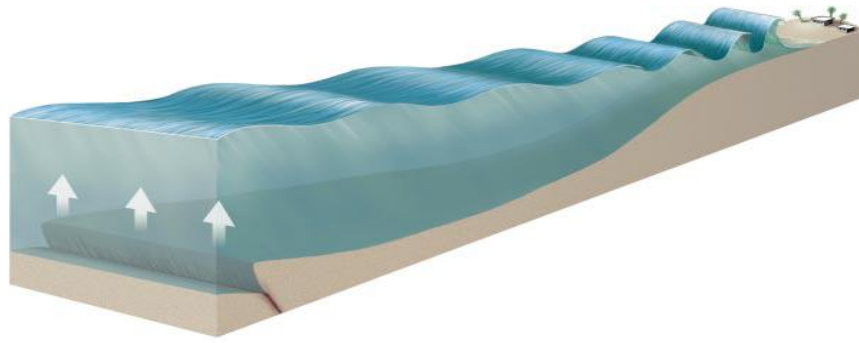


Figure 3 Displacement in the sea floor causing a series of travelling ocean waves (Gonzalez 1999).

As tsunami waves reach the shallow waters of the coast, the waves slow down and the water can pile up into a wall of destruction tens of metres or more in height. The effects can be amplified where a bay, harbor or lagoon funnels the wave as it moves inland.

In a tsunami, the whole water column from the ocean floor to its surface is affected, the initial disturbance creating a series of waves radiating outwards, until the waves either dissipate or collide with a shoreline (Fig 2). Very large sources (disturbances) are required to cause tsunami that are damaging at great distances from the source. For example, the magnitude (M) 9.5 Chile earthquake produced a 25 meter (m) high tsunami locally, over 10 m in Hawaii, and nearly 4 m at Gisborne in New Zealand. On the other hand, tsunamis that are generated locally do not need such a large source to be large and damaging at nearby shores. For example, the 1947 M7.1 earthquake off Gisborne affected 120 km of coastline, with a tsunami of 10 m maximum height occurring along tens of kilometers of coast north of Gisborne (Berryman 2005).

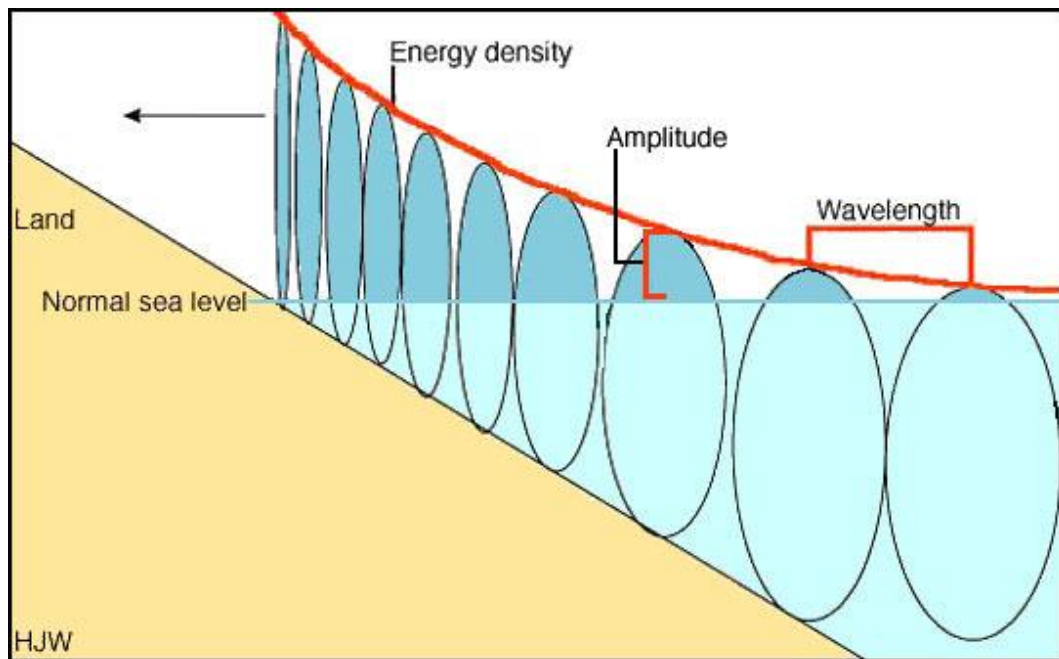


Figure 4 Wave energy of a tsunami wave in the form of an oval. If the oval does not touch sea bottom, the wave will barely rise above the normal sea level (shown light blue). The shallower the sea gets the higher the wave will rise before breaking

It is not necessarily the primary seismic event that affects coastal environments. For example, a distant fault rupture may have no impact, but the subsequent tsunami maybe devastating. Tsunamis tend to be the after-effects of seismic-related events or submarine landslides (mostly generated by earthquakes). Within the short period of human occupation, many parts of the country have undergone tectonic uplift or subsidence, as is evident in coastal areas by the presence of recently uplifted shorelines (Grapes & Downes 1997).

2.1 Historical Tsunami Events in Poverty Bay

The majority of tsunami occurring in New Zealand are caused by local sources. The largest tsunami occurring along the New Zealand coast have also been generated locally (de Lange and Healy 1986). These tsunami only affect a limited section of the coast (de Lange and Fraser 1999)

Off the East Coast of the North Island slope failure has occurred on a vast scale (Lewis *et al.* 1999). The largest failure in the Poverty Bay region, offshore from Ruatoria, involves over 3,600km² of sediment, which has collapsed as a blocky debris avalanche (Lewis *et al.* 1999).

Most large ($M_w > 6.5$) earthquakes in the North Island occurred prior to 1961, these events provide important information to supplement studies of more recent seismicity (Doser and Webb 2003).

Doser and Webb (2003) indicated that no large plate interface earthquakes have occurred in the central and southern North Island for the past 80 years (Figure 5), although six strike-slip earthquakes of $M_w \geq 6.8$ occurred within the Australian (upper) Plate during an extremely active 25 year period that began in 1917.

Only the $M_w > 7.2$ strike-slip events were associated with surface faulting, indicating the difficulties that may arise in attempting to identify active faults within this region. Two earthquakes ($M_w = 6.9-7.1$) off the north-eastern North Island in 1947 appear to have occurred along the plate interface and were associated with local tsunamis having run-up heights of up to 10 m (Doser and Webb 2003).

Two $M_w = 6.8$ events also occurred within the Pacific (lower) Plate, highlighting the hazards related to intra-slab events. Slip vectors for the earthquakes studied suggest that the majority of trans-current motion along the plate margin is accommodated within the Australian Plate, similar to the results obtained from studies of more recent, smaller earthquakes. Pure thrusting occurs along the plate

interface and T axes of intra-slab events indicate down-dip tension in the Pacific Plate (Doser and Webb 2003).

de Lange and Healy (1997) investigated the possibility of a tsunami by utilizing finite element modelling and indeed found that the 1947 tsunami was most likely generated by a slow shallow thrust earthquake effecting expulsion of diapiric material offshore. The source volume required to produce a 10 m wave was around 2.4 km³.

New Zealand's coastline is at risk from tsunami generated by either local or distant tectonic events. In historic times, seismic activity has ranged from barely detectable earthquakes and tsunami that caused no damage, to large-scale earth and sea movements capable of destroying cities and causing widespread regional disruption (e.g. 1931AD Napier earthquake (Hull 1986); 1947AD Gisborne tsunami (Eiby 1982)).

New Zealand sits astride the boundary between two major tectonic plates, the Australian and Pacific, it is to be expected that locally generated earthquakes would have impacted on the prehistoric inhabitants of the country. Also, since the sea has been at or near the present level for some 7000 years, there will undoubtedly have been larger magnitude and less frequent events that have affected coastal environments prior to human occupation.

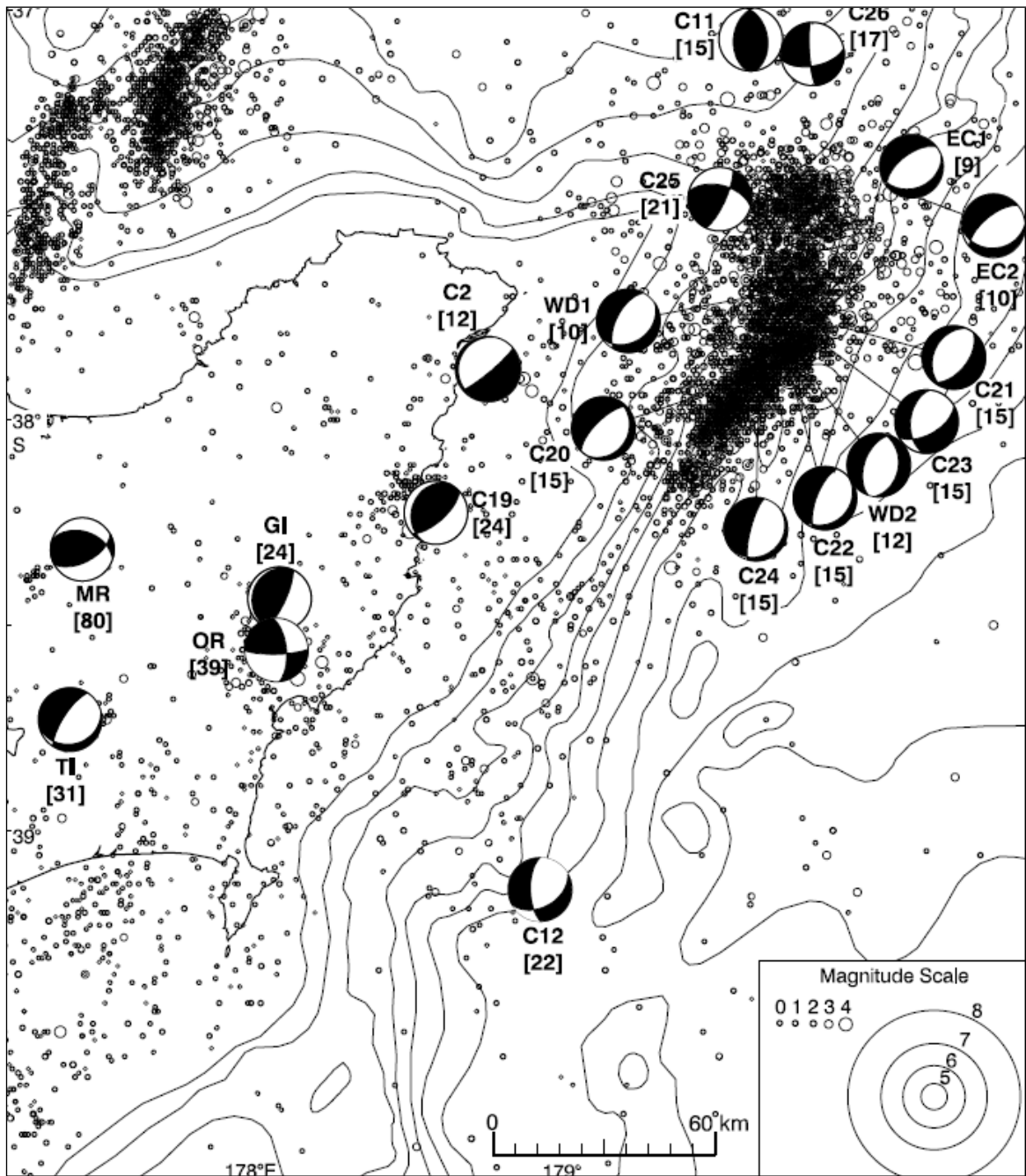


Figure 5 Recent seismicity (1990–1999) of the Poverty Bay region (Doser and Webb 2003) The letters next to the balls are event labels given by Doser and Webb to identify individual earthquakes i.e. GI = Gisborne and the numbers in brackets i.e. [31] is the depth of the earthquake event.

2.2 Tsunami Caused by Fault Dislocation

There is considerable uncertainty about how tsunami earthquakes produce large tsunamis (de Lange 1998)

Earthquakes generate about 90% of all tsunamis (Lockridge 1990). However, this is not the only mechanism that generates tsunami they can also be generated by submarine volcanic explosions, by submarine landslides or subaerial landslides plunging into the water, or, most commonly, by tectonic displacements of the ocean floor associated with earthquakes (Ayre 1975; Lockridge 1990). The latter is what will be covered in this thesis.

Seaquakes or submarine earthquakes are one of the main energy sources of tsunami generation (Velichko *et al* 2002). To predict the height of tsunami waves along the coast, it is necessary to know the parameters of disturbance of the ocean in the zone of a seismic event (Velichko *et al* 2002).

Some of the locally generated tsunamis that may have occurred at Gisborne may have been generated by marl diapirism (mud volcanoes) (Parnell *et al* 1999). This isn't surprising considering the tectonic activity and gas hydrates that have been found off-shore of Gisborne around Aerial Bank. However this type of tsunami generation is beyond the scope of this thesis and will not covered.

It is already known that tectonic fault dislocation has the ability to cause tsunami waves. As can be seen in figure 3, if a section of tectonic plate becomes disjointed and either drops or is thrust upwards there will be a resulting disturbance in the water surface above that point. This displacement will cause an in-balance in the water which will try and get back to equilibrium; this in turn causes a sudden rush of water either away from or toward the area of disturbance and thus can cause a tsunami wave.

2.3 Earthquakes and Tsunamis

The largest earthquakes often occur where the ocean floor is being carried down into the Earth's interior (figure 6). During a large earthquake beneath the ocean floor, the floor is displaced both vertically and horizontally. Although horizontal displacements are often larger, they are unimportant for tsunami generate except to the extent that the sloping ocean floor also forces a vertical displacement of the water column.

Upward displacements in one area are approximately balanced by downward displacements elsewhere, because Earth is close to incompressible, so the wave troughs are as important as the crests. The displacement of the water happens rapidly relative to the time it would take for a wave to disperse the resulting ocean surface displacement. Even though the tsunami speed may seem fast, it is slow compared to the time scale of the earthquake rupture.

When thinking about an earthquake there is more to it than just the epicentre, as the net ground displacement isn't just confined to a small region. There are three length scales to consider. The largest of these is the length of the rupture; in the Sumatran earthquake this was approximately 1200km and extended along a gently curving line. Offshore of Gisborne the March 1947 rupture length was approximately 90km.

Earthquakes begin at a particular point in the rupture surface and then propagate, like the propagation of a crack, though they typically take advantage of a zone of previous rupture. The rupture speed is a few kilometres per second or less, somewhat less than the propagation speeds of shear waves in rock. The intermediate length scale is the width of the rupture zone and is perpendicular to the length.

The area (Length x Width) is of great importance in defining the magnitude of the quake. The smallest but nevertheless important length scale is the net displacement that occurs on the rupture surface during the quake.

Chapter Two – Literature Review

Large and small earthquakes differ primarily in the size of the area of rupture and not the stresses or stress drop. The standard magnitude scale (Richter scale) is based on the base ten logarithm.

Immediately after a tsunamigenic earthquake the ocean surface is disturbed over roughly the same area as the area of the rupture surface. The energy in a tsunami is considerably lower than the energy in the earthquake that created it. The wave propagates away from the initially disturbed area and the polarity of the wave (whether the first arrival is a crest or a trough) depends on the location of the affected coastline relative to the original disturbance.

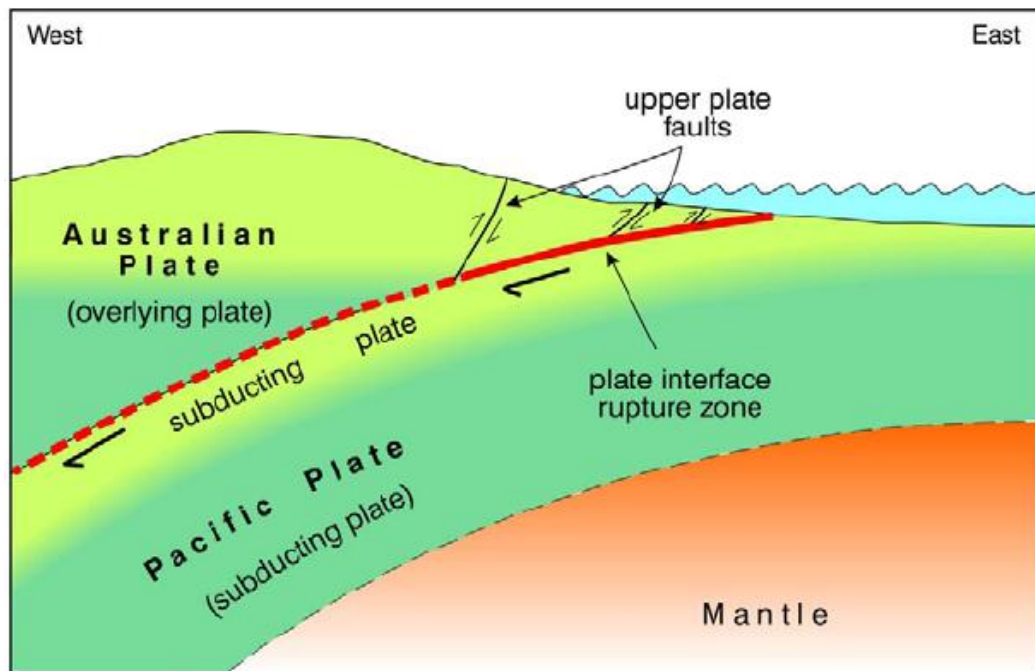


Figure 6 Seismic cross section through the Hikurangi subduction zone (Berryman 2005)

2.4 Tsunami Problems for Gisborne

Gisborne is unfortunate in the sense that its geographical location lends itself to a higher risk of a tsunami inundation from both, distant (Chile) and local source (Kermadec trench) events.

The continental shelf between Mahia Peninsula and East Cape along the east coast of the North Island of New Zealand is narrow and drops steeply into the Hikurangi Trench, making it similar to the setting of the Saundaun Tsunami of 17 July 1998. Two tsunamis with maximum heights of 8-10 m were generated in this region in 1947, associated with earthquakes with $M_L < 6$, $M_w 7 - 7.2$ (deLange 1998)

Both earthquakes exhibited features characteristic of tsunami earthquakes including a predominance of long period energy, a large discrepancy between the surface wave magnitude and other magnitude measures, and an association with a large thickness of weak sediments close to a subduction zone. Similar tsunami have been reported in 1908, 1927-28 and 1970, but with no known associated seismic event (deLange 1998).

Numerical modelling of the 1947 events indicates that the tsunamis were generated from the southern and northern ends of Ariel Bank, within the location errors of the reported earthquake epicentres. Ariel Bank overlies at least one large marl diapir. Numerical modelling also indicates that relatively small volumes of material are required to generate the large waves seen, the travel times are of the order of quarter of an hour, and that resonance occurs in Poverty Bay and between the coast and Ariel Bank. It is concluded that this region of coast has the highest tsunami hazard for New Zealand for the following reasons:

- 1) Explosive release of material from marl diapirs appears to have relatively short return periods ($1 < 150$ years);
- 2) The only warning of local tsunami generation are the ground motions associated with the rupturing of strata overlying the diapirs. These motions are weak, and some historic cases have been aseismic (deLange 1998).

Chapter Two – Literature Review

Poverty Bay is exposed to the southeast, whilst being protected by Young Nicks Head to the south and Tuaheni Point to the northeast. The bay is 8.5 km wide at its entrance and is bordered by 13.4 km of mainly sandy beaches interrupted by the mouths of Wherowhero Lagoon and Waipaoa River (Carter *et al* 1997).

The Poverty Bay Flats are very low lying. This can be seen from recent LiDAR (2005) data that was flown over the bay and also the frequency of flooding.

Port Gisborne is the central hub of exports for goods produced in the area, so therefore it is of great concern what could happen to this infrastructure in the event of a tsunami. The Port is enclosed within a harbour and breakwater system in the north of Poverty Bay, New Zealand (Fig 7) Since historical development in the 1880s, it has experienced ongoing coastal engineering problems relating to wave exposure, siltation within the port, extensive dredging requirements, as well as resonance within the confines of the present harbour (Whyte, 1984).



Figure 7 View of Port Gisborne, log handling area and breakwaters

Chapter Two – Literature Review

The localised effect of resonance can substantially modify the incoming tsunami wave train at any locality along the coast or in harbours and estuaries. Each part of the coast (bays, harbours, ports or river mouths). If an arriving tsunami wave-train comprises wave periods (time between wave crests) that match the natural resonance periods of the locality or region, these wave periods will be selectively “picked out” and amplified causing higher wave heights and run-up at the shoreline and continuing excitation of the water body, compared with other locations where there is no match up with the natural resonance frequency (Environment Waikato Technical Report 2004)

This resonance effect has been seen before in tidal data from Gisborne harbour in relation to the 1960 Chilean tsunami (Heath 1982). Thus there is an increased risk to the port.

The main harbour response to tsunamis is generally that of the quarter-wavelength resonance (depending on the harbour dimensions), although at Lyttelton and possibly other east-coast ports, a continental edge-wave response is evident — this latter response possibly involves the Chatham Rise, extending 1000 km perpendicular to the east coast of South Island, acting as a three-quarter wavelength (Heath 1985).

2.5 The Human Impact

The human impact of a tsunami is evident from the 2004 Boxing Day event in Indonesia. People were unaware of the risk that they faced and also the extent of the damage that would be caused by such an event.

This is not only true for the people affected in Indonesia but also for people in New Zealand and more so Gisborne. The general public has limited knowledge of tsunami risk in their area (Pishief 2006). For distantly generated tsunami sufficient warning should be able to be given from the Pacific Tsunami Warning Centre (PTWC) but there is no real warning system in place in New Zealand for locally generated events.

At the Richard H. Hagemeter Centre (PTWC), the operational center of the Tsunami Warning System in the Pacific (TWSP), scientists monitor seismological and water level stations throughout the Pacific Basin, evaluate potentially tsunamigenic earthquakes, monitor tsunami waves and disseminate tsunami warning information (Karling 2005).

There are other problems also facing the east coast region. Due to the spread out nature of some of the neighboring communities i.e. Tolaga Bay, Tokomaru Bay, Te Aroha, emergency response is logistically difficult.

Tsunamis strike coasts and penetrate inland, creating conditions hazardous to both people and property in a zone which is particularly valuable for housing and certain economic activities. The hazard from tsunamis can be computed, based on two factors; (1) the probability that a tsunami of X runup height and Y inland inundation distance will strike a coast, and (2) the extent of human use of the same stretch of coast (Morgan 1984).

Because of the difficulties in broadcasting short-term warnings due to damaged infrastructure and the very short time period to take action, it is critical that all people in hazard areas immediately recognize that the earthquake is their warning and take immediate response.

Chapter Two – Literature Review

This involves a complicated set of behaviors — protecting oneself during the earthquake, identifying the earthquake as an event capable of producing damaging waves, identifying one's location as hazardous, knowing how to get to a safe area, and how long one must remain away from the coast before the danger period is over.

All of these actions must be taken in the absence of any official guidance and during a time of extreme personal duress. The diverse population of coastal regions further complicates this problem. Information about the tsunami risk and appropriate response needs to be communicated to residents, workers (seasonal and year-round), regional visitors, and transient populations, all of whom have different exposure to the tsunami hazard (Dengler 1998).

The difficulty lies in attempting to unravel the impact that these events have had on coastal environments when the further back one works in time, the less well-preserved the record becomes. Prior to the collation of the historic record, evidence for earthquakes is found primarily from fault trenching and geological interpretation of the sediments. This is of little use to our understanding of the impact of catastrophic events on coastal environments other than providing a chronology of large, local earthquakes that can be correlated with anomalous features in the sedimentary record of coastal wetlands (Chague-Goff 2001).

CHAPTER 3 – Fault Mechanism &

Earthquakes Affecting Gisborne

3.0 Introduction

New Zealand lies within a complex zone of deformation between the Australian and Pacific Plates. In the North Island the Pacific Plate is being subducted beneath the Australian Plate along the Hikurangi Trough (Doser and Webb 2003).

The intracontinental transform zone (where the Pacific and Australian plate meet) links, via the Alpine Fault of the South Island, to an opposite facing zone of oblique collision and subduction south-west of New Zealand (Lewis 1998).

There are many faults that lie off-shore of Gisborne that have the potential to cause local tsunami through earthquakes and submarine landslides (Figure 8). The thin lines directly offshore of Gisborne (GN) on figure 8 shows the 2 main fault zones (shaded) that have potential to cause a locally generated tsunami.

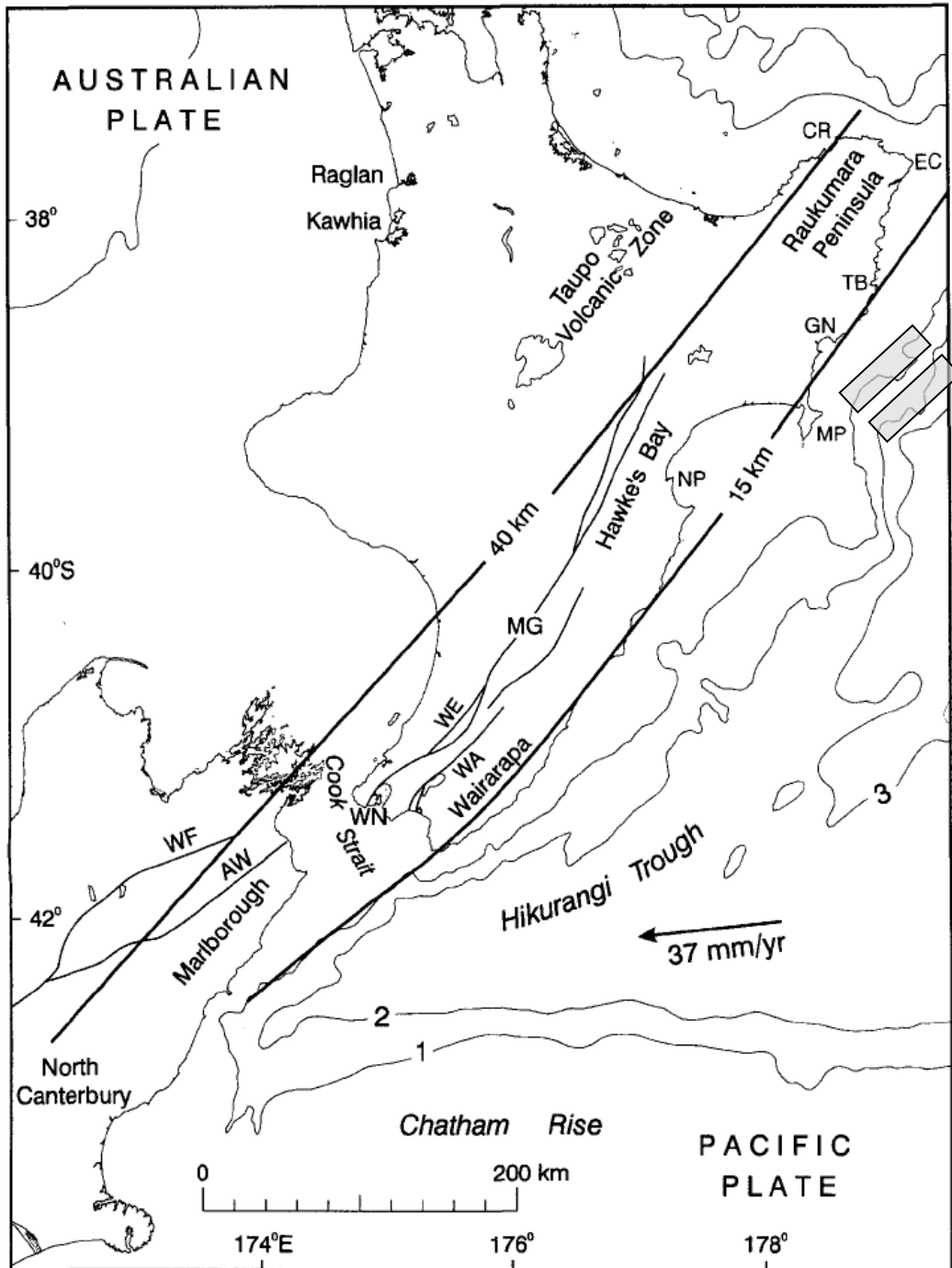


Figure 8 Tectonic setting of the Hikurangi subduction zone. The heavy contours are isobaths of the shallow part of the plate interface. Thin lines are active faults, the shaded area is the fault used for the earthquake simulation. The arrow shows the velocity of the Pacific plate relative to the Australian plate. AW . Awatere Fault; CR, Cape Runaway; EC, East Cape; GN Gisborne; MG, Manawatu Gorge . MP, Mahia Peninsula; NP, Napier. TB, Tolaga Bay; WA, Wairarapa Fault; WE, Wellington Fault; WI Wairau Fault; WN, Wellington (Rayners 1998)

3.1 Faults off East Cape

The Hikurangi Trough, off eastern New Zealand, is at the southern end of the Tonga-Kermadec-Hikurangi subduction system, which merges into a zone of intra-continental transform. The trough is mainly a turbidite filled trench, but includes an oblique collision, fore-deep basin. Its northern end has as sharp boundary with the deep, sediment starved, Kermadec Trench (Lewis 1998).

Webb and Anderson (1998) have observed a partitioning of motion along the Hikurangi margin, with strike-slip faulting occurring above the plate interface and pure thrusting occurring along the plate interface.

Deployments of portable seismographs along the Hikurangi subduction zone have provided insights in the structure and seismic strain regime of the subducted and overlaying plates, and the nature of plate coupling at the shallow part of the plate interface (Doser and Webb 2003; Reyners 1998).

The seismogenic zone appears to be located along the shallowly dipping part of the plate interface deeper than 15km (McGinty et al 2000). Reyners (1998) has suggested that the seismogenic zone decreases in down-dip width from about 70km in the Wellington region to about 20km in the northern part of the Raukumara Peninsula, and that the degree of coupling of the plates also decreases from strong to weak (Fig 9).

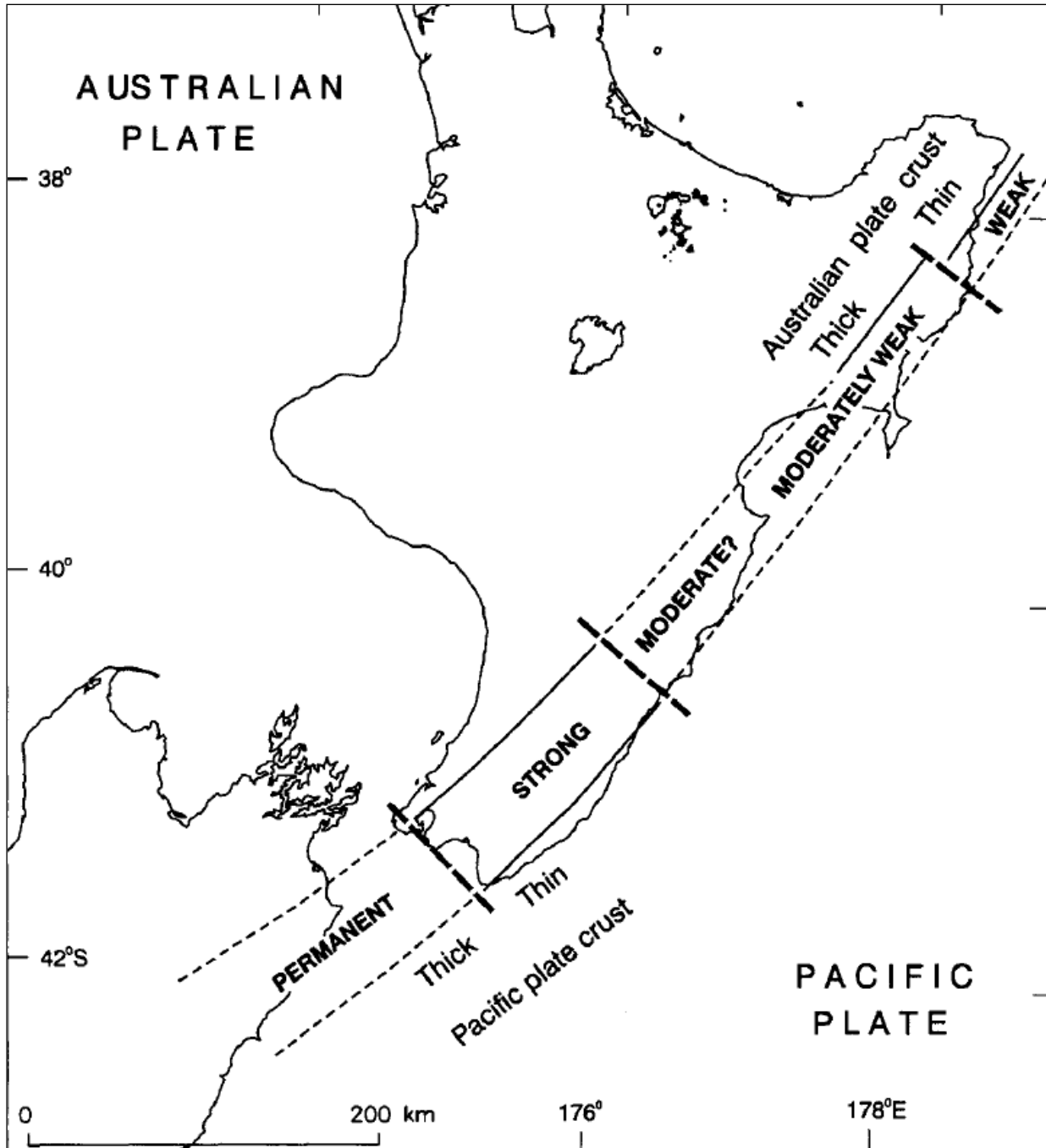


Figure 9 The inferred locked portion of the plate interface (seismogenic zone) along the shallow part of the Hikurangi subduction zone together with the interpreted degree of coupling. Boundaries of the locked zone are shown dashed where more uncertain. Thick dashed lines denote boundaries of segments of the locked zone suggested by tomographic inversions of earthquake arrival time data for 3-D crustal structure.

There is concentrated activity in the 10-20km depth range on the lower part of the overlying plate, between Ruatoria and Tolaga Bay as well as in the uppermost part of the subducted plate between Te Karaka and Gisborne (Rayners et al 1999).

Previous studies of focal mechanisms in the Raukumara Peninsula have mostly involved bodywave modelling of infrequent larger events in the Mw 5.6-6.2 range (Webb et al. 1998). The Mw 5.6 event of 1966 and Mw 5.8 event of 1992 are both located close to the plate interface and have low-angle thrusting mechanisms, consistent with interplate slip (Webb et al. 1998).

There have also been three other substantial earthquakes that occurred in the subducted plate. The T axes of the Mw 5.9 earthquake of 1985 and Mw 6.2 earthquake of 1993, which occurred at 31 and 39 km depth respectively, align closely with the local dip of the subducted plate. However, the 80 km-deep 1984 event (Mw 5.9) has a T axis plunge that differs from the local slab dip by 36° , and an azimuth which is 16° from the downdip direction (Webb et al. 1998).

An estimation of the size of possible subduction thrust events is hampered by a lack of information on the location of the seaward end of the locked zone (Rayners 1998). Assuming that the area near Gisborne is the same as in the Wairarapa region (i.e. 15 km deep), the width of the locked zone decreases progressively to the northeast to be only 20 km wide in the northern part of the Raukumara peninsula. This decrease in width is due not only to a decrease in depth of the downdip limit of the locked zone, but also to an increase in the dip of the plate interface to the northeast (Rayners 1998).

3.2 Fault Characteristics and Focal Mechanisms

The average dip of the locked zone beneath the northern part of the Raukumara Peninsular is 12° (Reyners and McGinty 1999). Reyners (1998) calculated that Mw 6.9 would be likely for a subduction thrust event of the northern part of the Raukumara Peninsula. This size event is within the range of magnitudes that is capable of causing a tsunami from a submarine landslide.

The focal mechanisms of small earthquakes determined by Reyners and McGinty (1999) suggest a change in the strain regime of the overlying plate with depth, with trench-ward extensional strain in the upper 9.5km changing to trench-ward compressional strain in the lower part of the plate and at the plate interface.

The focal mechanism of the Mw 5.6 Gisborne earthquake of 1966 is also favored by the stress regime if slip occurred on the steeply dipping nodal plane aligned along the margin. Although this event had many aftershocks, they were too poorly recorded to define a fault plane. However, as this event occurred close to the plate interface and has the other nodal plane aligned with the interface, it has in the past been interpreted as involving interplate slip (Webb et al. 1985).

For the purpose of this thesis, a past earthquake event that is known to have preceded a tsunami has been chosen to model. (P1) in figure 10 is related to the March 1947 earthquake that was associated with a tsunami. This event was located offshore beneath the continental slope (Downes et al. 2000).

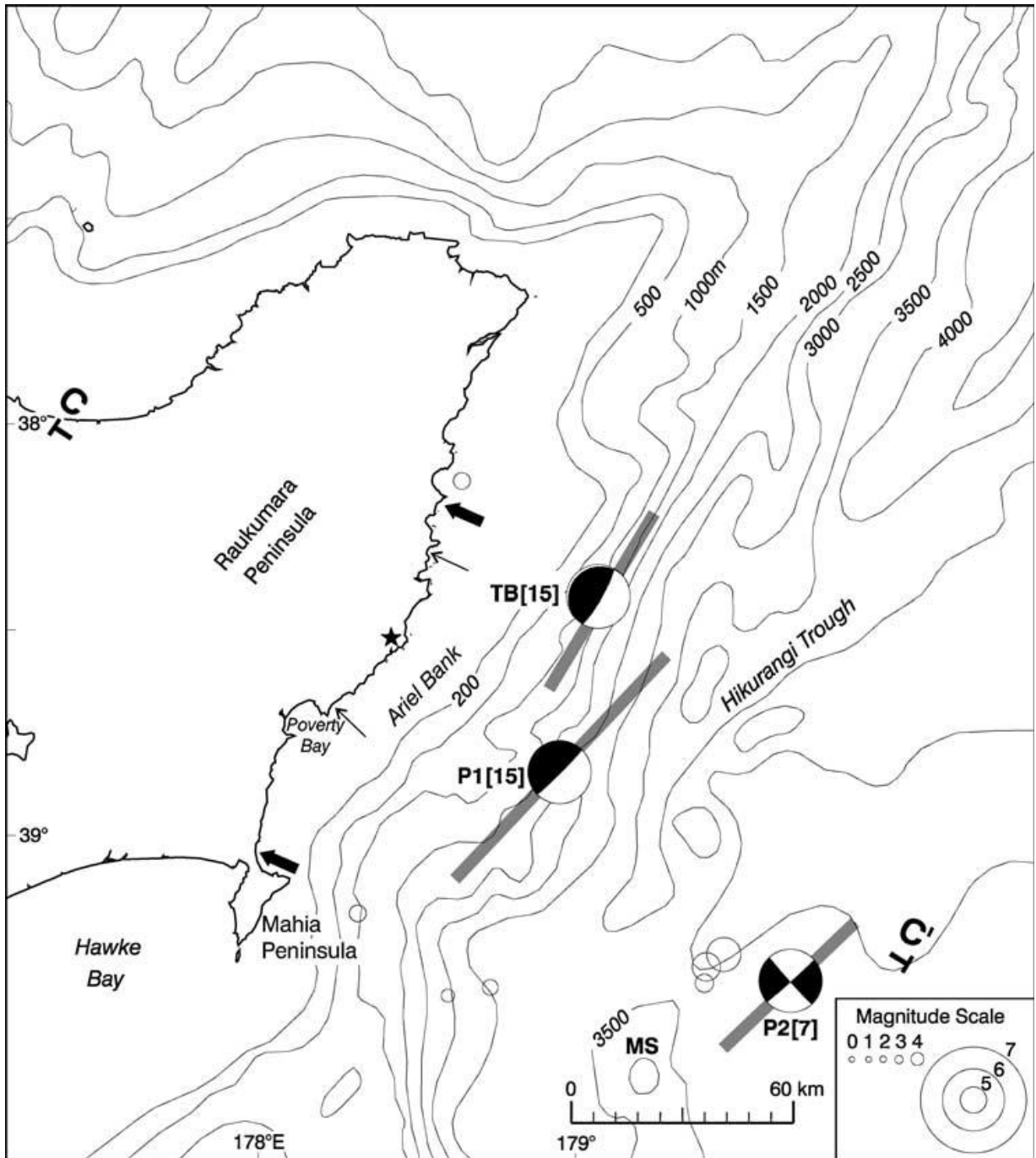


Figure 10 Historical seismicity of the Poverty Bay region. Circles are relocated aftershocks of the 1947 earthquake sequence (Downes et al. 2000). The arrows show the northern and southern limit of the coastline where the tsunami runup height exceeded 1 m in 1947 March (bold arrows) and 1947 May (fine arrows) (Downes et al. 2000). The asterisk denotes the region where the tsunami runup height exceeded 10 m in 1947 March. MS denotes Mahia Seamount. Grey bars indicate rupture lengths determined from the rupture duration for $M_w > 6.5$ earthquakes within the Pacific Plate (P2) or along the plate interface (P1, TB) (Doser and Webb 2003).

The Centroid Moment Tensor (CMT) solution of the earthquake (P1) was:

Event	Strike	Dip	Rake	Moment x 10¹⁸ Nm	Depth (km)	Slip
March 1947	225±30	3±5	90±30	51±5	15±5	315

(Doser and Webb 2003)

This earthquake in Poverty Bay is associated with a tsunami and exhibits many of the characteristics of a ‘tsunami’ earthquake. The focal depth and focal mechanism is consistent with slip on the plate interface.

Rupture and fault segmentation during the events may be controlled by a change in the crustal structure of the Australian Plate that appears to give rise to changes in the strike of the coastline and in the offshore bathymetry.

Seismic reflection data collected by Collot *et al.* (1996) indicates that the Mahia Seamount is in the process of being subducted beneath the plate margin, which also could contribute to rupture complications for events occurring along the plate interface. Slip along the shallow portion of the plate interface is consistent with the geodetic studies of Arnadottir *et al.* (1999).

CHAPTER 4 – Numerical Modeling

4.0 Introduction

Numerical modelling of tsunamis is commonly carried out to better understand events that have occurred either during or before historical times. Numerical modelling can also help to predict the effects of a future tsunami.

In this thesis, the hydrodynamic model 3DD was used to simulate the generation and propagation of tsunami.

4.1 Numerical Modelling of Tsunami

All hydrodynamic models are based on two equations, which are solved by time stepping. These equations are the momentum and mass conservations equations. The momentum equation is used to describe the accelerations and retardation of the water body when forces are applied to it. The equation is based on Newton's 2nd law of motion, where the acceleration is directionally proportional to any force acting upon it. The mass conservation equation determines the total mass entering and leaving model cells and ensures that mass is conserved in these cells (Black 1995).

The tsunami modelling process can be divided into three parts: generation, propagation, and run-up (Liu et al. 1991; González 1999).

Tsunami generation and run up are more difficult to model with computer simulations (González 1999). Simulation of wave run-up is very important for assessing the magnitude of flooding in coastal areas (Grilli and Watts 1999). Wave run-up depends on both the wave amplitude and the wave period (Watts 1998). It is the main objective of this thesis to determine wave run-up and how it will affect the Gisborne region.

One common characteristic of all run-up laws that Tadepalli and Synolakis 1994 found is a square root dependence on the slope, and an almost linear dependence of the run-up on the wave height 'H'.

The process involved in tsunami generation is extremely complex (Harbitz et al 1993). It is generally assumed that the sea-surface displacement is identical to that of the ocean bottom (González 1999).

Numerical modelling of tsunami is often carried out using a finite-element grid (Prasetya 1998; de Lange and Prasetya 1999). A finite-element grid consists of polygons of unequal size. The polygons are scaled by the time taken by waves to travel across each of them. Therefore, the polygons situated in deep water are larger than those situated near the coast (Tinti et al 1999a). This style of grid is suitable for marine basins with irregular coastlines (Tinti et al 2000) and is also a more efficient use of computer capacity (Kienle et al 1987).

4.1 3DD Hydrodynamic Model

The hydrodynamic model 3DD uses momentum and continuity equations to determine current speeds, current directions and water levels for both deep and shallow water simulations. The model can be run in two or three dimensions (Black 1995).

Information is supplied to the model through an information file and the model output is written to disk at intervals selected by the user (Black 1995). The model 3DD can also generate time series of current speeds, directions and water level for specified cells at every time step.

There are a range of support tools that 3DD utilises to aid in the preparation of input files and extraction of results. The main graphics and diagnostic program is PLOT3DD written by Dr Richard Gorman (NIWA). PLOT3DD is a Matlab support routine that uses data obtained in 3DD to generate plots as vector plots, time series plots, and three dimensional projections. These plots can be generated for a variety of different variables and at different scales (Black 1995).

Nested model simulations are also used due to the size of the grid and the need for a high resolution closer in the bay. 3DD uses a “nested grid” program which extracts boundary information from a coarse grid run and places the information in formatted boundary files for finer grid simulations (Black 1995).

The momentum equation in two-dimensions applied in the model is given by Black (1993) as:

$$\frac{\partial u}{\partial t} + \frac{u\partial u}{\partial x} + \frac{v\partial u}{\partial y} - fv = -\frac{g\partial\zeta}{\partial x} - \frac{1\partial p_{atm}}{\rho\partial x} + \frac{\rho_a\gamma W_x|W|}{\rho(d+\zeta)} - \frac{gu(u^2+v^2)^{1/2}}{C^2h} + A_H\left(\frac{\partial^2 u}{\partial x^2} + \frac{\partial^2 u}{\partial y^2}\right)$$

$$\frac{\partial v}{\partial t} + \frac{u\partial v}{\partial x} + \frac{v\partial v}{\partial y} - fu = -\frac{g\partial\zeta}{\partial y} - \frac{1\partial p_{atm}}{\rho\partial y} + \frac{\rho_a\gamma W_y|W|}{\rho(d+\zeta)} - \frac{gv(u^2+v^2)^{1/2}}{C^2h} + A_H\left(\frac{\partial^2 v}{\partial x^2} + \frac{\partial^2 v}{\partial y^2}\right)$$

Where t is the time, u and v are vertically-averaged velocities in the x , y directions respectively, h is the total water depth, d is the depth below sea level datum, ζ is the water level above a horizontal datum, g is the gravitational acceleration, f is the Coriolis parameter, p_{atm} is the atmospheric pressure, A_H is the horizontal eddy viscosity coefficient, ρ is water density, W is the wind speed at 10m above water level W_x and W_y are the x and y components of wind speed, γ is the wind drag coefficient and ρ_a is the density of air (Black 1983). C is Chezy's C given by Black (1995) as:

$$C = 18 \log_{10}(0.37h/z_0)$$

Where z_0 is the roughness length. Over sandy beds the value of z_0 is typically between 0.001 and 0.003, but roughness lengths as large as 0.08 can be used over coral. A constant roughness can be used over the entire grid or one value for roughness can be entered for each cell in the same format as the bathymetry. All terms in the momentum equation have accelerations units ($m.s^{-2}$) (Black 1995).

Chapter Four – Numerical Modeling

The mass conservation equation in two-dimensions is given by Black (1983) as:

$$\frac{\partial \zeta}{\partial t} + \frac{\partial}{\partial x} (d + \zeta)u + \frac{\partial}{\partial y} (d + \zeta)v + 0$$

The Courant number provides a lower limit for the model time step size. The Courant number is given by (Black 1995) as:

$$\Delta t < \frac{\partial x}{\sqrt{2gh}}$$

The model grid used in 3DD is made up of evenly spaced, rectangular cells. Each cell is referenced by an (i,j) coordinate. The x direction (U velocity) is positive to the east and corresponds with increasing i and the V velocity is positive to the north and corresponds with increasing j . The cell (1,1) is located at the bottom left corner of the grid and the maximum coordinates ($IMAX, JMAX$) are located at the top right corner Black (1995).

The bathymetry is entered into the model in the form of an ASCII file as the depths in the mid-point of each cell. The depths are entered in metres and are positive downward from the water surface. The water depths in land cells are entered as -9.0, which indicate an impermeable boundary. Intertidal zones are input as negative depths which are larger than -9.0 the model grid can also be rotated (Black 1995).

Chapter Four – Numerical Modeling

Various other features are available in 3DD. A sponge boundary can be applied to an open boundary to damp out water propagating out of the grid and to reduce reflection. The sponge is give by Black (1995) as:

$$\zeta_i = \left((i - i_b) / N \right)^r (\zeta_i - \zeta_b) + \zeta_b$$

Where ζ_i is the sea level at grid cell i . ζ_b is the value in the boundary cell, N is the number of cells in the sponge and r is a constant. Latitude can be input into the model to calculate the Coriolis force. The latitude is negative in the Southern Hemisphere. The effects of barometric pressure and wind can also be entered into the model as a time series (Black 1995).

CHAPTER 5 - Methodology

5.0 Introduction

This chapter describes the processes involved to create the files and steps necessary to complete the hydrodynamic modelling of a tsunami for the Gisborne region. Several software applications were utilised for bathymetry manipulation and tsunami propagation modelling.

The software used included:

1. Arc GIS 9.1
2. Golden Software SURFER6
3. 3DD
4. MapInfo
5. MatLab
6. QuickTime

The chapter will also conclude with a discussion of the treatment of errors and how these were overcome.

5.1 Bathymetry Construction

High resolution bathymetric data from the continental shelf into the coast is not often collected due to the time, money and area involved to get such data. Only small portions of the New Zealand continental shelf are known in sufficient detail to recognise and count all the submarine landslides there (Berryman 2005).

Poverty Bay has not been extensively surveyed before, and the available soundings (bathymetry) that have been collected are relatively dated i.e. the navy fair sheets that were used were surveyed between February and April in 1986.

Therefore, the bathymetry data used for the numerical modelling was constructed by digitising LINZ hydrographic charts and Navy Fair sheets for the Poverty area.

Figures 11 and 12 show the difference between a normal un-digitised chart and a chart that has been digitised. Figure 12 has been “Geo-referenced” to the New Zealand coastline with a known coordinate projection; New Zealand Map Grid (NZMG). Therefore any points that are placed on the map are assigned an X, Y coordinate in relation to the New Zealand coast.

LINZ charts NZ55 and NZ1356 were used to get a broad coverage of bathymetric points, but due to the large spatial variation of these points they didn’t give high enough resolution to allow for accurate hydrodynamic modelling. This was a problem as it would have a major effect on the accuracy of the results.

Navy Hydrographic Fair Sheets were used to try and fill in some of the more critical areas, such as in closer to the shore where the hydrodynamics start to become more complex due to the shallowing water and the presence of rocky outcrops and areas of dredge spoil. As tsunami enters shallow water it undergoes shoaling transformations similar to those affecting swell and surf. These can alter tsunami characteristics considerably (de Lange *et al* 1999).

The Navy Fair Sheets were produced in February of 1980 and all maps were from index 5613 and incorporated chart numbers 27 -34. Bathymetry was corrected from the charts to mean sea level (MSL), by subtracting 1.09m from all the data that was digitised off both Navy Fair Sheets and LINZ Hydrographic charts.

LiDAR data was also utilised, which provided high resolution bathymetry on land. The Airborne Laser Scanning (ALS) data was acquired from a fixed wing aircraft between October 17th-18th and on October 27th and November 23rd 2005. Delays in acquiring the data were due to low cloud over the bay.

Chapter Five – Methodology

The LiDAR data set contained over 20 million points, which made the computational time to manipulate and alter data very long. Therefore, the data was smoothed to 5m resolution in ArcGIS; this helped decrease the size of the bathymetric files and speed up the processing time. Once the data had been digitised off of the Navy Fair sheets and the LINZ hydrographic charts, the data points were exported as ASCII files and merged together as one text document that could be read into SURFER6 and plotted as bathymetric maps as seen in Figure 13.

LINZ Hydrographic Chart - NZ55

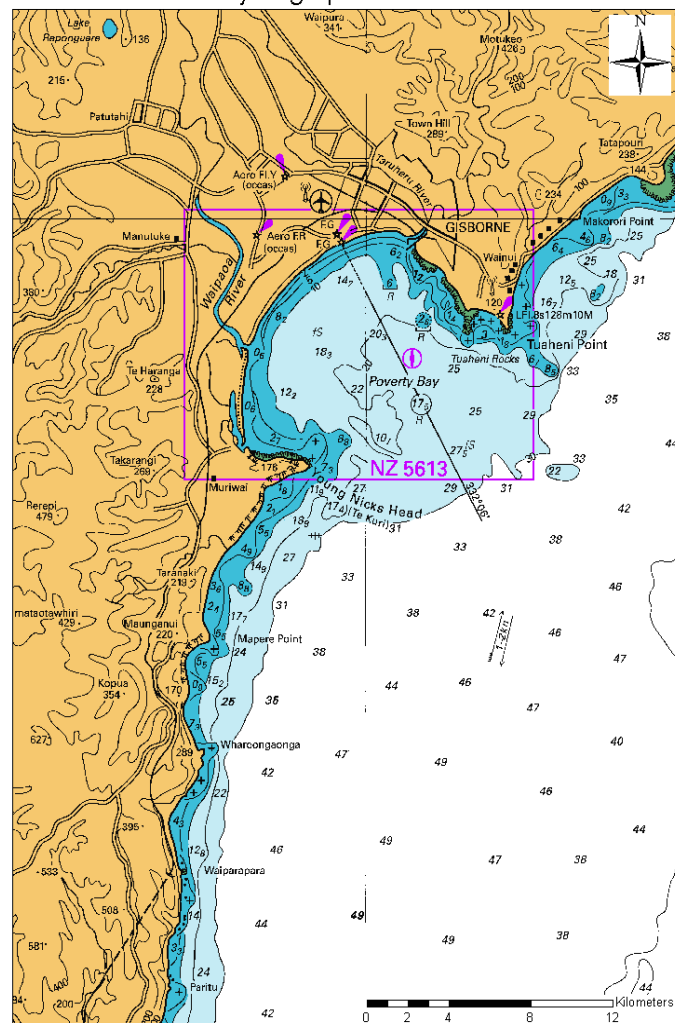


Figure 11 LINZ Hydrographic Chart NZ55 before digitisation

Digitised LINZ Hydrographic Chart - NZ55

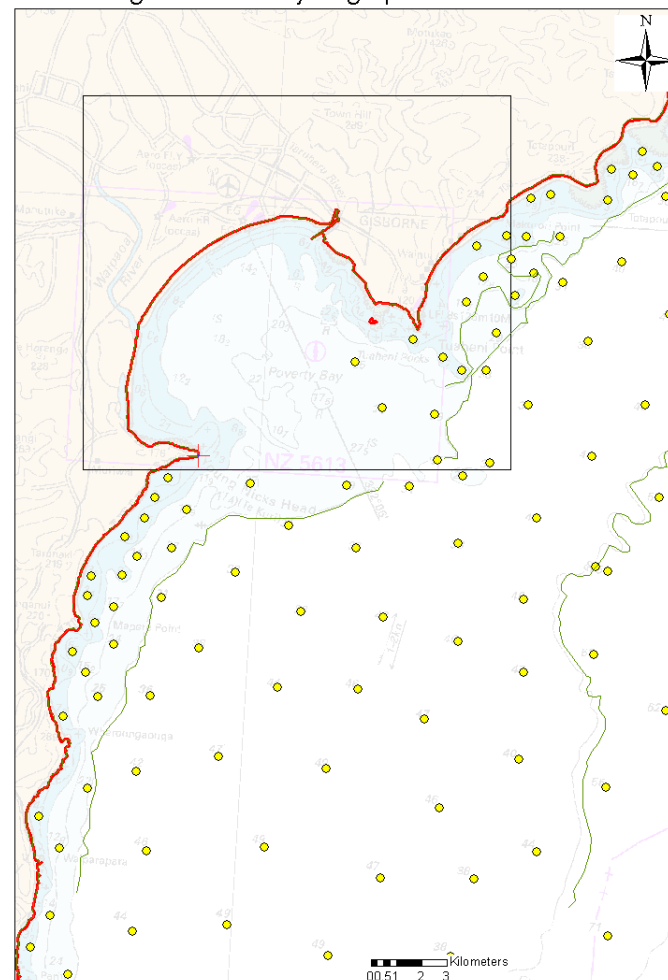


Figure 12 LINZ Hydrographic Chart NZ55 after digitisation.

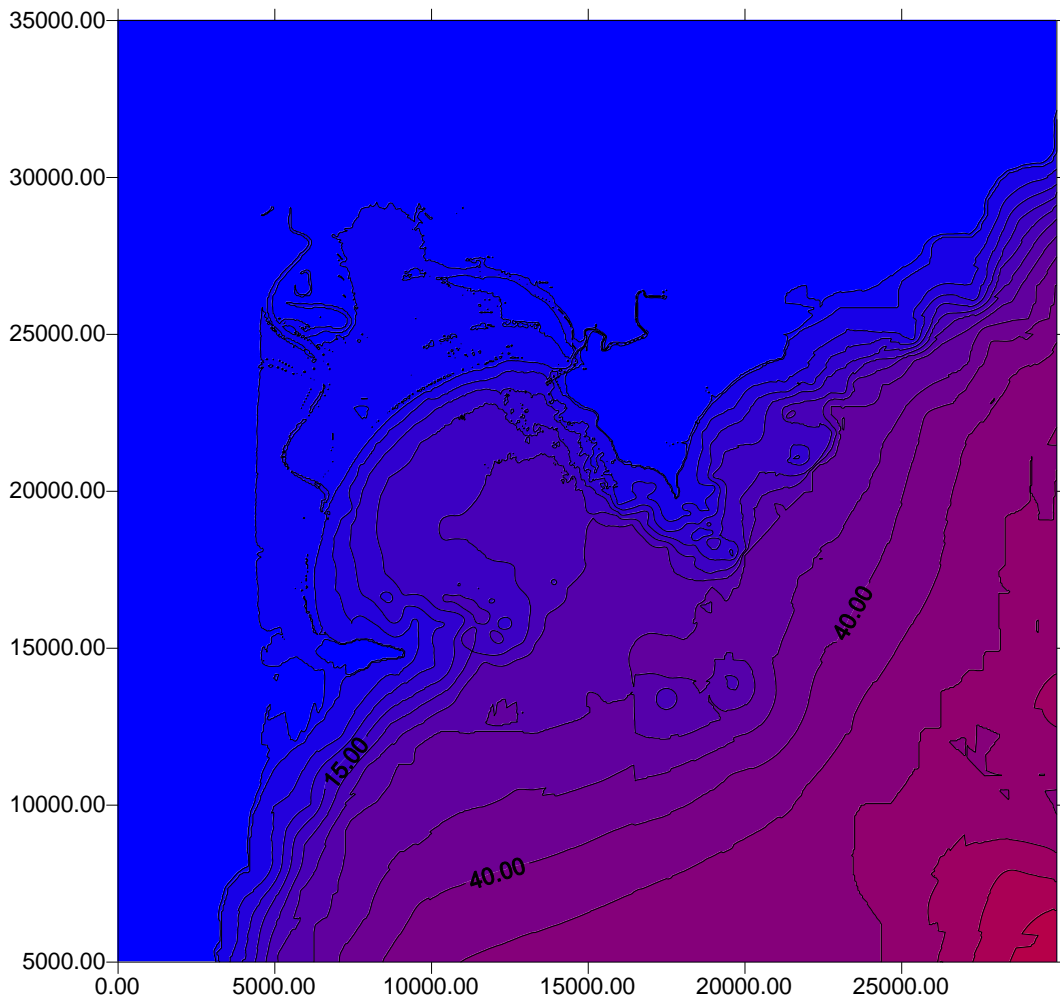


Figure 13 Bathymetric map at 150m spacing produced in SURFER6 using both digitised data and LiDAR data.

Every chart digitised had its own individual bathymetric text file, this not only made it easier to keep a log of which charts had been digitised, but also aided in keeping file sizes to a more manageable size.

MapInfo was used to manipulate the digitised data and merged all the individual files into one, which was in turn loaded into SURFER6 that created the bathymetric files and maps that would be used in the 3DD numerical modelling suite.

5.2 Tsunami Generation

The tsunami generation location was chosen due to the history of the area and past events. As seen in chapter 3, figure 11, Doser and Webb 2003 have plotted historical earthquake events that have preceded tsunami waves that are known to have caused damage to the Poverty Bay/East Cape region in May and March of 1947.

The source of the tsunami event that was used in this thesis was sourced parallel to the entrance of Poverty Bay. It was generated along the same fault that has already generated tsunami events in the past, so therefore, it is not unrealistic to assume that it could happen again. The location of the earthquake position chosen for this thesis has been further supported with the December 20th 2007 earthquake that struck 50km south east of Gisborne at a depth of 31km and magnitude of 6.6Mw (Figure 14). This seismic event was approximately 20km north west of the modelled location.



Figure 14 Map showing historical earthquakes >Mw 5 for the Gisborne Region. Red-star indicates the December 20th 2007 Gisborne Earthquake, Black-star indicates model simulation location (adapted from GNS 2007 image).

5.3 Fault Dislocation Parameters / Initial Condition

Two different fault dislocation scenarios were used (FAULT A and FAULT B); the location used was the same for both events however the magnitude of the dislocation was altered. Both faults are reverse dip slip faults. FAULT B was bigger than FAULT A; this was done to see what, if any difference in wave characteristic and inundation pattern could be seen.

The fault dislocation model was created following “The displacement fields of inclined faults” paper written by L. Mansinha and D.E. Smylie 1971. The paper looks at closed analytical expressions for the displacement fields of inclined, finite strike-slip and dip-slip faults. Their equations were used in the numerical computation of the displacement fields used in this thesis.

The displacement field theory has been generalised to real Earth models by Mansinha and Smylie (1971). They included initial hydrostatic stress, a liquid core, self-gravitation, and radial variation of elastic constants, density and gravity (Mansinha *et al* 1971).

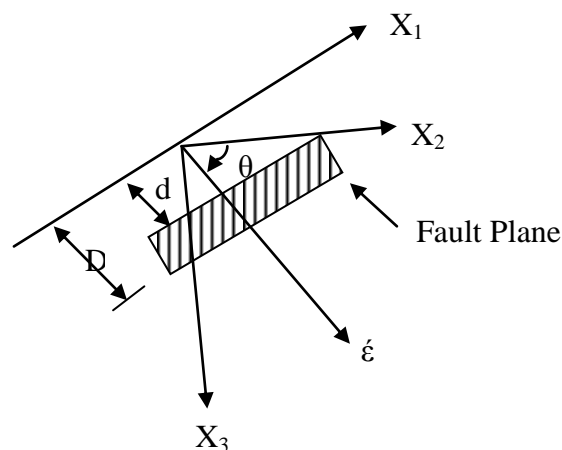


Figure 15 Fault geometry and coordinate system adapted from Mansinha *et al* 1971

Chapter Five – Methodology

X_1 , X_2 and X_3 – Are components of displacement from the source point of the earthquake. X_1 is displacements along the fault, X_2 is displacement away (out) from the fault and X_3 is downward displacement.

Θ – The dip angle of the fault.

D – is a range of distance, in this case it measures the amount of displacement from X_1 to the outer edge of the Fault Plane.

d – similar to D in that it measures a range of distance, however, here it determines the amount of displacement from X_1 to the inside edge of the Fault Plane.

These variables come together to form the displacement field produced by a dislocation across a surface.

FAULT A:

Start point along Fault axis X=126000.000 Y=119000.000

End point of Fault axis X=103000.000 Y=79000.000

Length of Fault (km) 46.141 (km)

Angle between N and Fault Axis (deg. CW) - 215.000

Width of Fault (metre) - 10000.000 (m)

Focal depth (metre) - 10000.000 (m)

dip angle (degree) - 25.000 (°)

slip angle (degree) - 110.000 (°)

f displacement (metre) - 20.000 (m)

20.000 (m)

Height of initial Wave (metre) 5.551 (m)

Maximum positive amplitude (metre) 4.382 (m)

Minimum negative amplitude (metre) -1.169 (m)

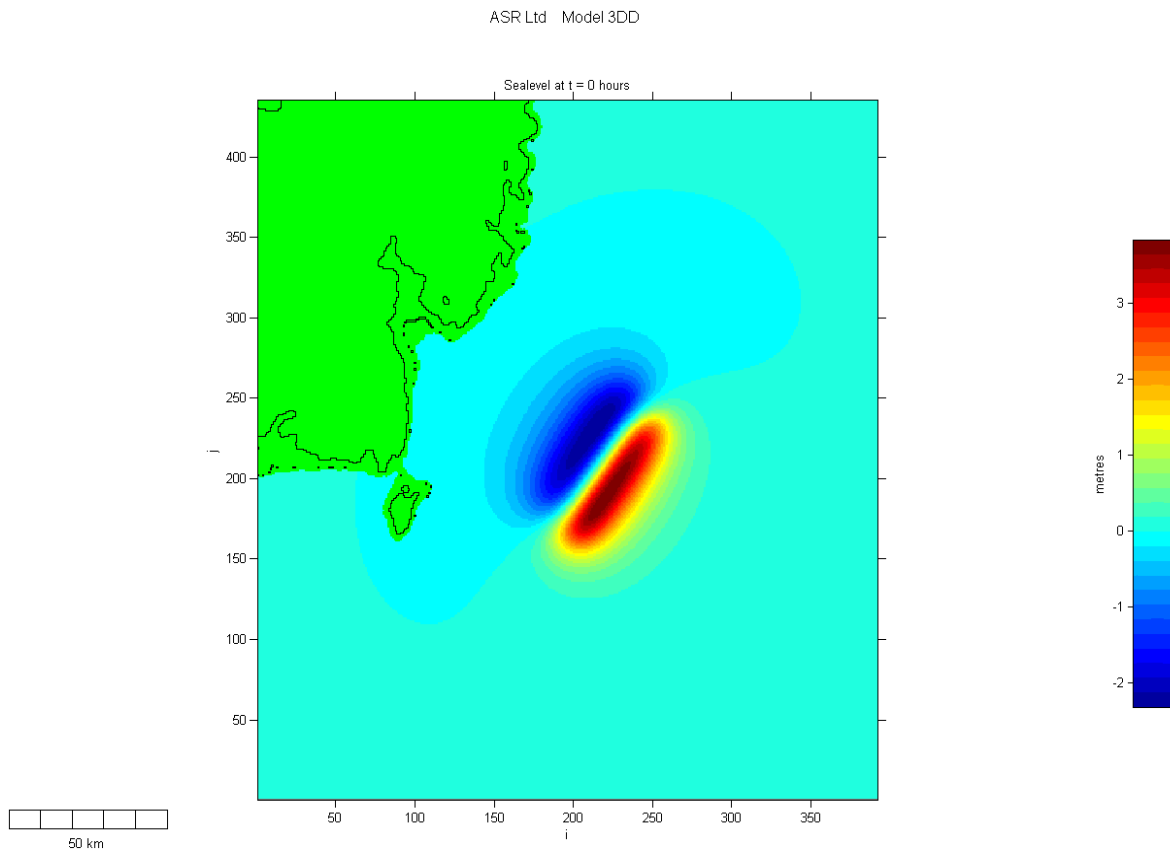


Figure 16 Initial conditon FAULT A

FAULT B

Start point along Fault axis X=126000.000 Y=119000.000

End point of Fault axis X=103000.000 Y=79000.000

Length of Fault (km) 46.141 (km)

Angle between N and Fault Axis (deg. CW) - 215.000 (°)

Width of fault (meter) - 10000.000 (m)

Focal depth (meter) - 10000.000 (m)

Dip angle (degree) - 10.000 (°)

Slip angle (degree) - 110.000 (°)

f displacement (meter) - 20.000 (m)

20.000 (m)

Height of initial wave (meter) is 6.158 (m)

Maximum Positive amplitude (meter) 3.839 (m)

Minimum Negative amplitude (meter) -2.319 (m)

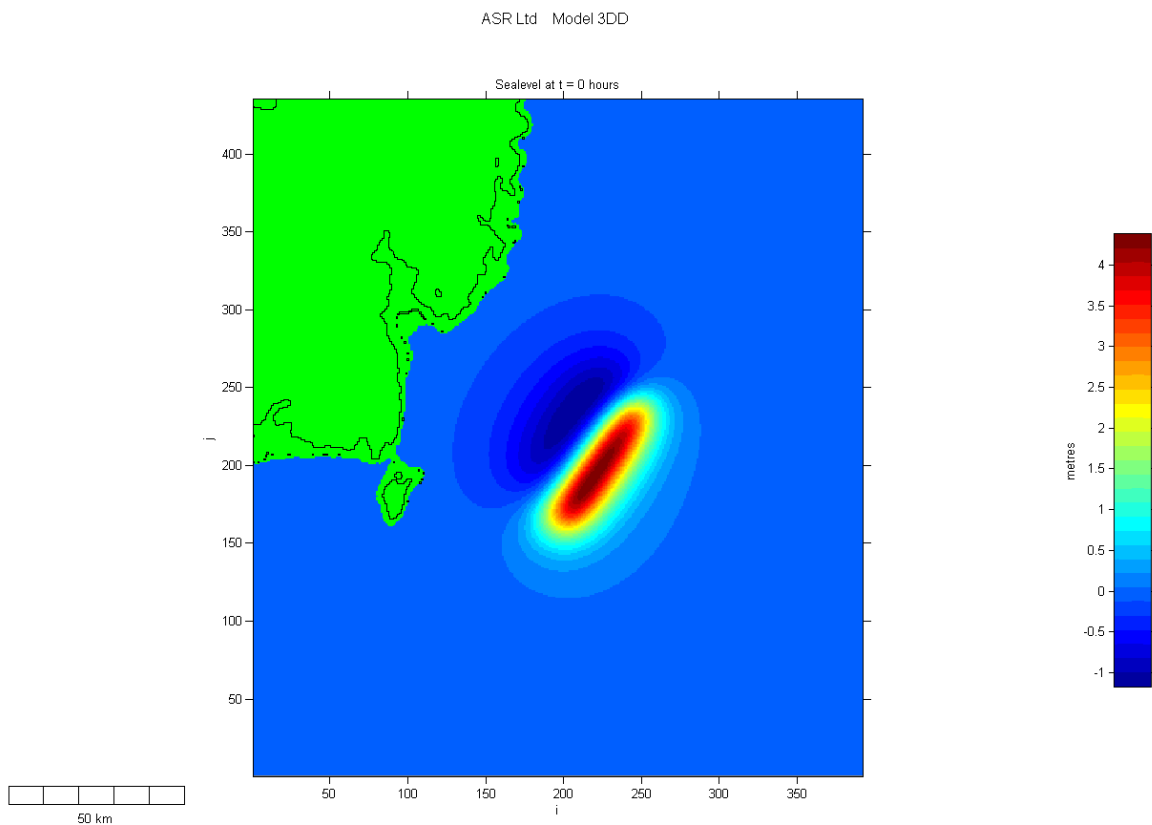


Figure 17 Initial condition FAULT B

5.4 Model Run Set-up

The faults made dislocation models that were used as the initial condition for the computer models. All the necessary variables were input into the 3DD Hydrographic interface i.e. bathymetry files and boundary files and the models were left to run until they had 6hrs of model time saved.

The first model run was done with a coarse (500m) model grid that had very low resolution and minimal detail. This wouldn't be acceptable enough as the objective of this thesis is to try and get as accurate as possible inundation limits. Therefore, grid nesting had to be carried out in order to get the grid size down and the resolution higher.

This involved re-gridding XYZ bathymetry and LiDAR data at smaller grid spacings. The grid spacings used for this thesis were 500m, 150m, 50m and 15m.

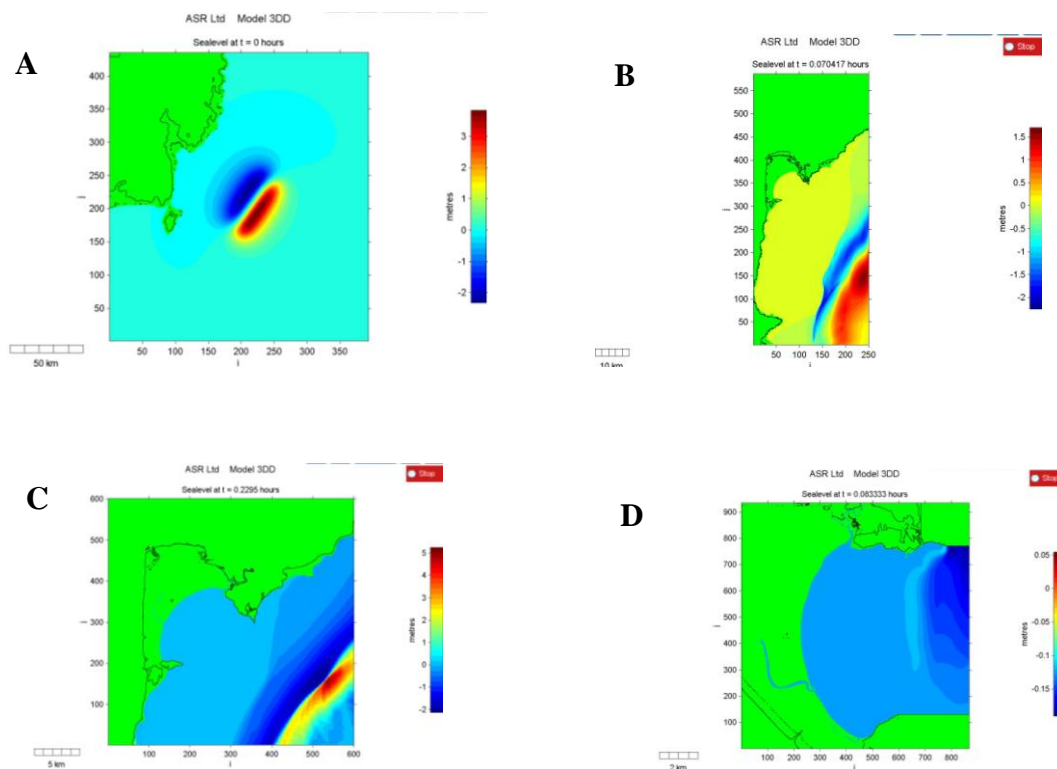


Figure 18 Four nested model grids A-500m, B-150m, C-50m, D-15m

3DD support tools were used to create the boundary files for each subsequent model run. This required finding an origin point within the new small grid that referenced back to the larger grid; so known locations e.g. headlands (Young Nicks Head) were used or any other known point on each map. The reason this had to be done was due the re-gridding and cropping, each time the grid was refined, it changed the origin compared to the larger grid.

The origin is a very important part to get right, as the model won't run if it is not lined up properly as you can get velocity values where there should be land values and vice versa. So the computer will be computing unrealistic values and thus crash.

Manipulation of the grids and boundaries was necessary in order to get model running, and also to gain the most realistic results. To help keep the model as stable as possible each time the new smaller grid was created it was cropped to try and minimise the number of boundaries and therefore minimise the complex velocity problems that were resulting.

An example of this is the final nested grid that was used. Due to the change in grid size from 50m to 15m the water velocities at the boundaries had very high velocities (as water from a 50x50m grid cell was trying to pass straight into a 15x15m grid cell) and in turn were causing the model to 'blow up' or crash.

A way around this was to rotate the grid 45° and block off a small part of the South and North boundary with land values, this was done using the "Depth Change" and "Rotate" function in 3DD support tools. By doing this the mouth of Poverty Bay was facing to the east and left only one open boundary to work with (Figure 20).

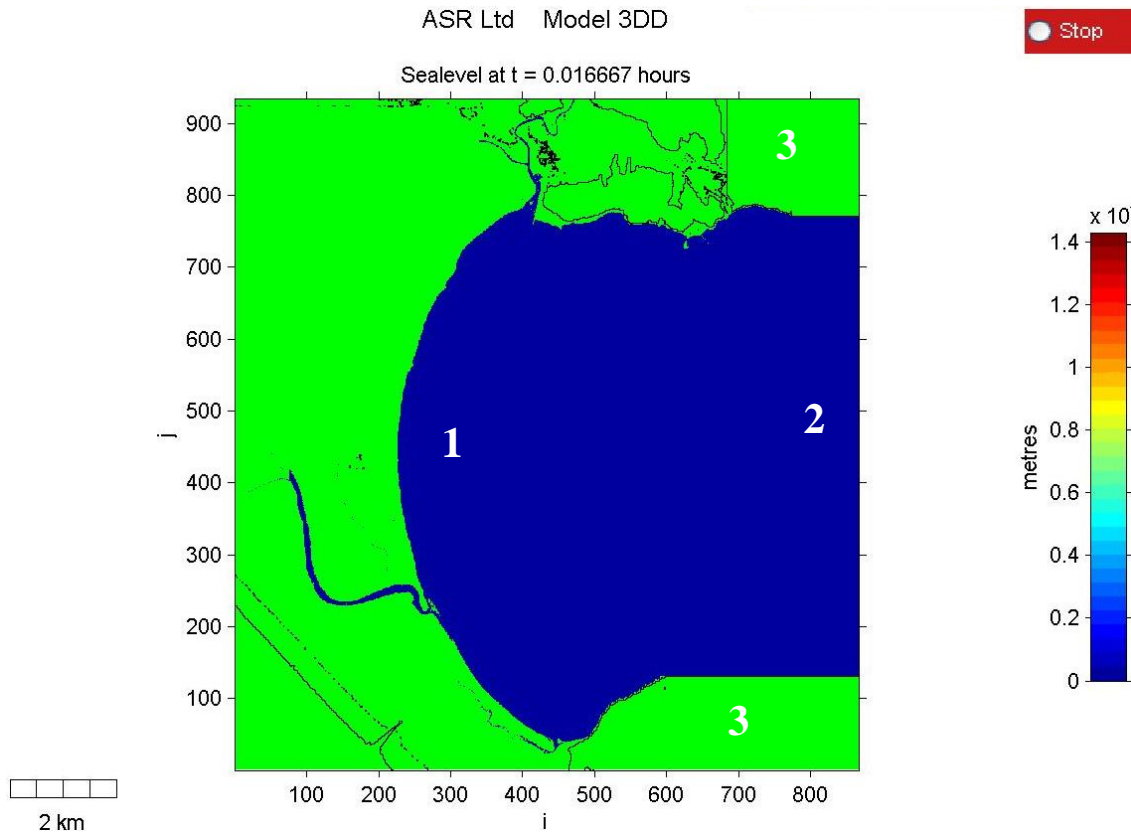


Figure 19 Rotated and depth changed 15m Grid

1. Showing the 45° rotation of Poverty Bay so that it is facing parallel to the East boundary.
2. Shows the only open boundary on the grid, the East Boundary
3. Shows the two small squares of land that were inserted to keep the grid to a single boundary and to minimise the complexity of velocities in confined spaces.

One other change that the 15m grid had to undergo was that of ‘setting the edges’ and putting a friction over the east boundary. This was another key to stabilising the model and getting it to run and obtaining the most accurate results possible.

Setting the edges allowed for a 10 cell wide strip of cells along the East boundary to be set to the same depth (an average of the depth for all the cells covered). This gave the wave velocities a uniform area to run into thus taking away the need for any excessive computations in velocities right on the boundary and in turn having it crash.

A friction layer was used over the whole of the bay, and was given a value 0.1 which gives the same friction acting on a wave as a sandy bottom would. This is fine as the whole of Poverty Bay leading into the shore is a gradual sloping sandy bed. A small strip of cells (10 cells wide) was set at a slightly higher bed friction of 0.5 for the length of the boundary. This helped to slow the wave velocities enough when they were coming in, and along with the uniform boundary assisted the wave to stabilise and propagate in without the model crashing.

5.5 Image Outputs and Animations

The final step was to create the animation movie files was made by utilising Plot3DD in MatLab and QuickTime. Picture files of each time step for each grid were output in batch lots, once all the picture files had been saved individually they were then imported into QuickTime Player where they were could be saved as a continuous movie file.

This helped to get a clearer picture of what was going on, as it created a seamless movie file of the tsunami wave propagating into the bay.

CHAPTER 6 - Results

6.0 Introduction

Model runs of two earthquake events (FAULT A and FAULT B) were simulated for a locally generated tsunami caused by an offshore earthquake.

The models show a tsunami wave approaching and starting to hit the East Cape 22mins and 16 minutes respectively after the earthquake event (Figure 21). This is in keeping with what has already been seen in Gisborne before with the March 1947 earthquake; a tsunami struck the coast approximately 25 – 30mins after the earthquake event (Eiby 1982).

The small difference in time could be contributed to the difference in location as not exactly the same location of the March 1947 event was used and also there was a difference in the generation mechanism for what has been said to have caused the March 1947 event.

As it has been suggested that there may have been three possible generation mechanisms, de Lange and Healy (1997) investigated the possibility of diapiric mechanisms being involved in tsunami generation for these two events. De Lange and Fraser (1999) suggested that these tsunami may also have been generated by slope failure triggered by the earthquake. This thesis, however, looks at earthquake fault dislocation, as the source.

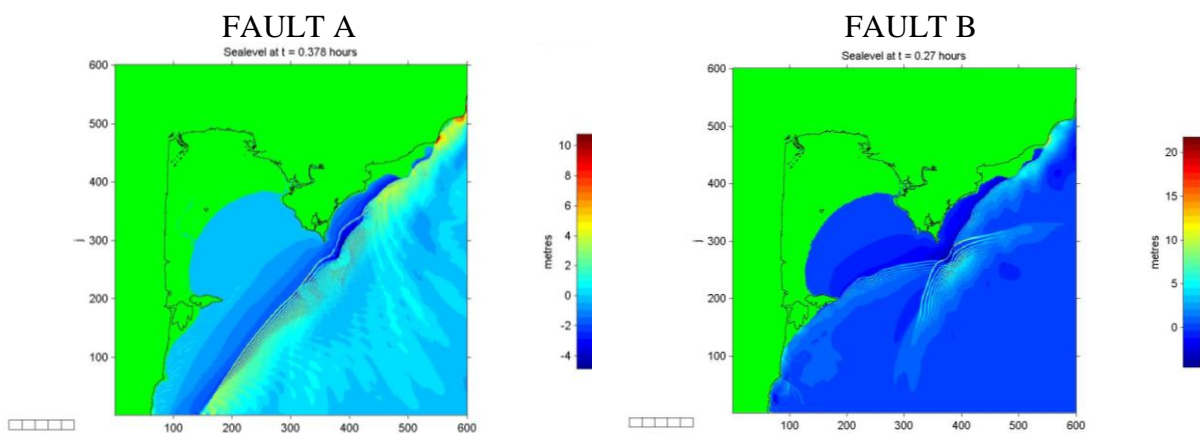


Figure 20 Time for tsunami to hit the Coast Fault A – 22mins Fault B – 16mins

6.1 Fault A Results

FAULT A tsunami has a longer travel time until it reaches the coast then FAULT B, this is due to the characteristic of the fault dislocation. The fault is a reverse fault which means for Gisborne the trough is the leading part of the tsunami, the resulting minimum negative amplitude is -1.169m with a maximum positive amplitude of 4.328m. The initial wave height is 5.551m.

Figure 21 shows a series of images of the tsunami wave propagating in towards the East Cape and Poverty Bay. The wave approaches parallel to the coast and therefore strikes the open coast first, i.e. Tatapouri, Makorori and Wainui (Figure 23), before it gets into the bay and causes any damage to the city.

Tatapouri is hit the hardest with an approximate wave height of 8m, this happens 26mins after the initial earthquake event (figure 23); such a wave height can be attributed to the focusing effect of ‘Aerial Bank’ focusing the wave’s energy in towards Tatapouri and the rocky outcrops that stretch out from the shore, aiding in the shoaling of the wave.

Aerial Bank is a shallow elongated area on the continental shelf (Katz, 1975). It is situated 15km offshore, parallel to the stretch of East Coast most severely affected by tsunami (Eiby 1982).

Since the wave is travelling parallel to the coast it runs straight into Poverty Bay. However it isn’t just a straight run in, there are two headlands that are either side of the Bay’s entrance; Young Nicks Head to the south and Tuaheni Point (Figure 2) to the north.

Chapter Six –Results

The tsunami first comes into contact with Tuaheni Point which causes the wave to refract and bend in towards the coast on the inside of the bay; this can be seen in image 3 of the sequence of figure 21. This also happens at Young Nicks Head.

The refracting wave off Tuahine Point along with the rocky outcropping reefs off of Kaiti beach, these can be seen in figure 22 the dark blue portion in the first image is where the reefs are located. This area is shallows a lot faster than the rest of the bay due to the reef and explains the water depth is -2m when the first wave hits as all the water is drawn away.

This rocky reef also aids in focusing the tsunami wave energy on Midway Beach and the city. These rocky outcrops are one reason that there is good surf waves at the town beaches, and they work best with long period waves such as a tsunami wave. The first wave hits the city shore 37mins after the earthquake event.

Another problem that seems to occur is the process of resonance within Poverty Bay (de Lange and Healy, 1997; de Lange and Fraser, 1999). This can be attributed to the dimensions of the bay and also the adjacent continental shelf (de Lange and Fraser 1999). This could account for the large wave and greater inundation that occurs 95mins after the earthquake event. However, the later waves in a tsunami form very complicated patterns, in which it is difficult to determine the relationship of a later wave to the initial source (Mofield *et al* 2004).

The total distance of city inundation is 1.15km along the beach. It stretches from the 'Cut' at Waikanae beach to Churchill Park on Centennial Marine Drive (Figure 22, right). The inundation reaches 200m inland from the sand dunes; this is the northern most extent of the yellow on (Figure 22, right). This incorporates the main section of housing and camping ground.

A street map incorporated with a FAULT A inundation image (figure 28) has been included to show the areas of inundation in relation to street names.

Chapter Six –Results

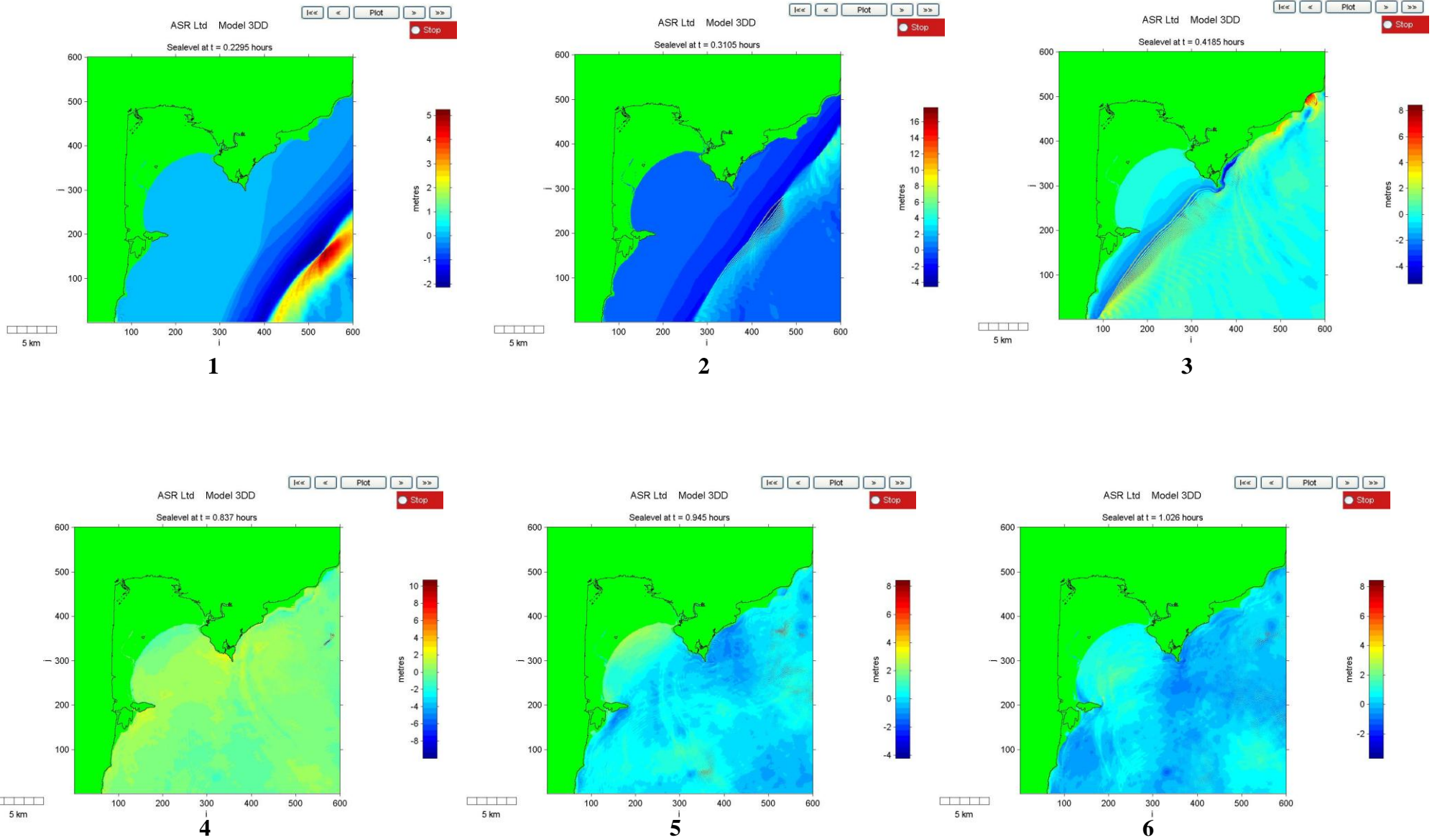


Figure 21 Fault A Image Sequence of a Tsunami wave hitting the East Cape and Poverty Bay

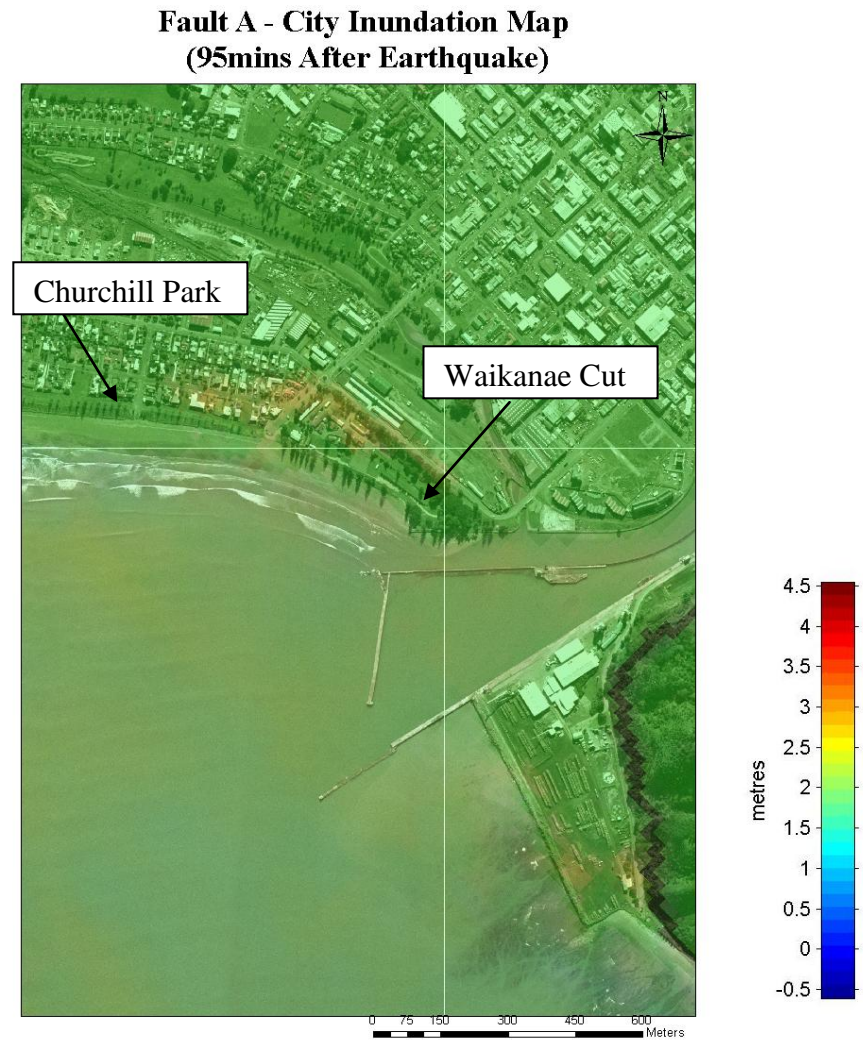
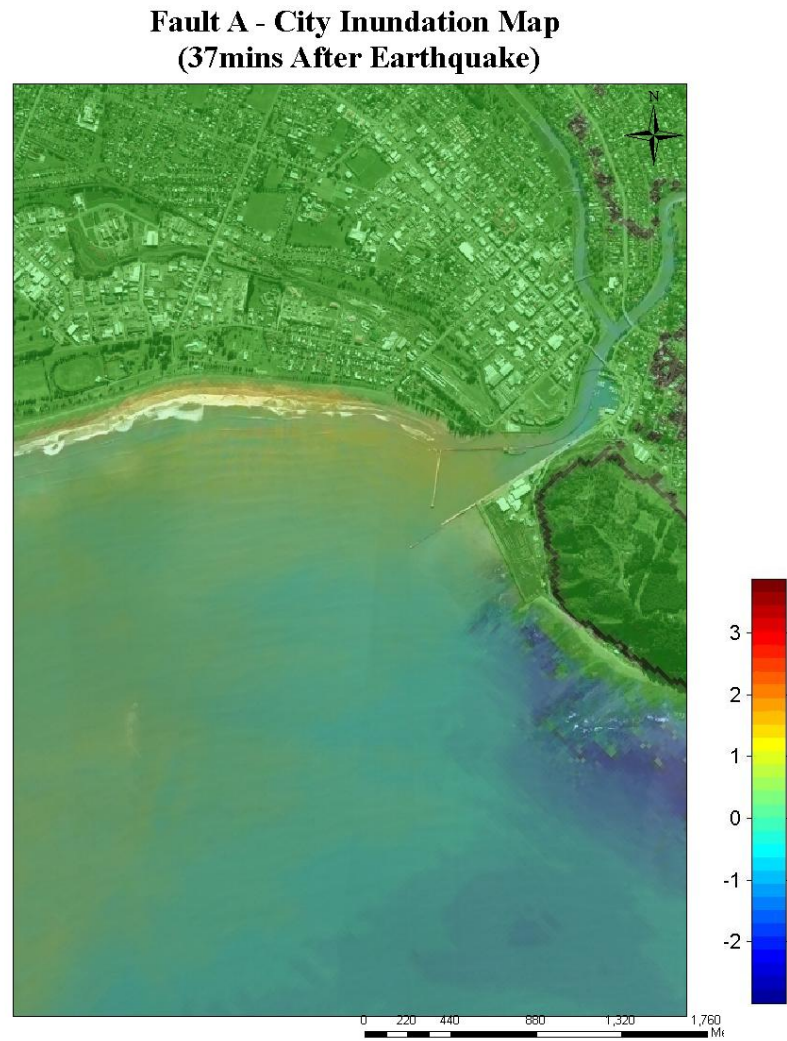
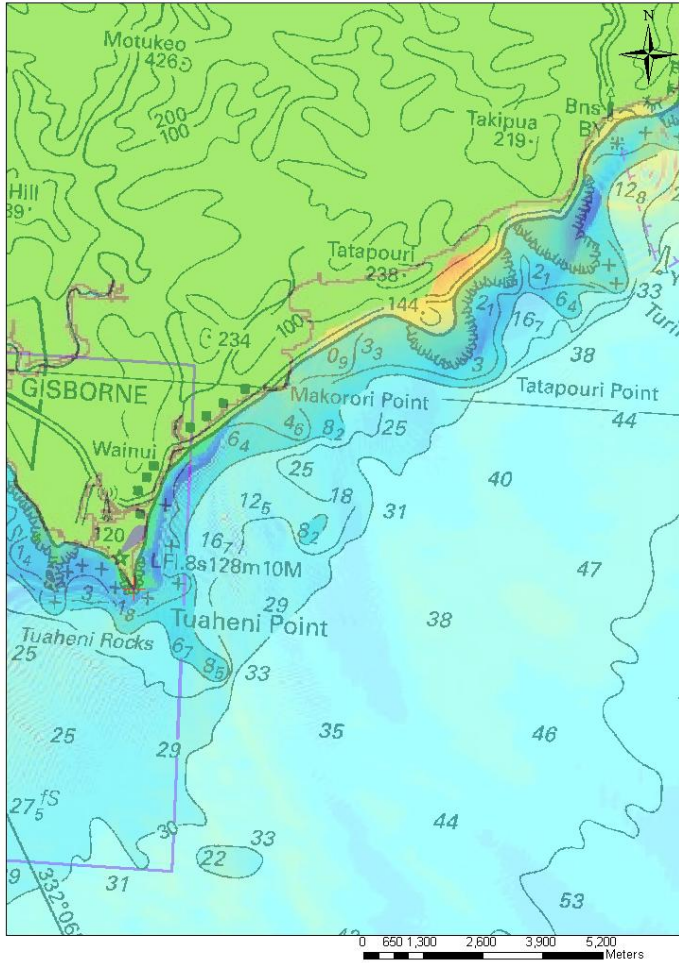


Figure 22 Inundation maps for the city from FAULT A, left shows the wave as it hits and right shows the full extent of inundation for FAULT A (Both images are overlay on Terralink International 2005 Ltd satellite images)

**Fault A - Coastal Inundation Map
(26 mins After Earthquake)**



**Fault A - Coastal Inundation Map
(28 mins After Earthquake)**

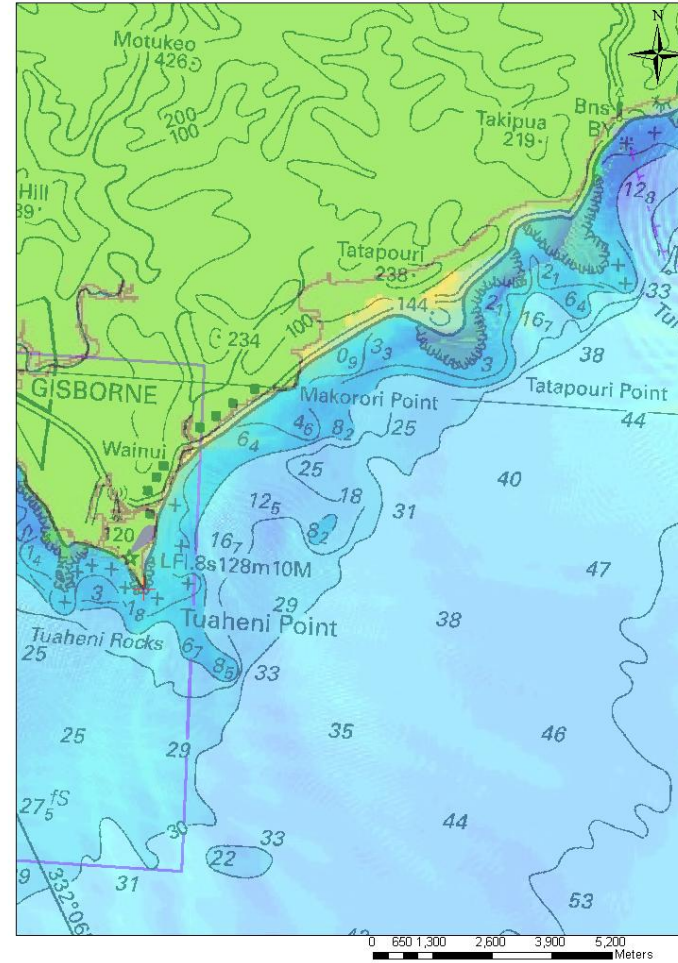


Figure 23 Inundation maps for the coast from FAULT A, left shows the wave as it hits and right shows the full extent of inundation for FAULT A

6.2 Fault B Results

FAULT B had an initial wave height of 6.1m with a maximum positive amplitude of -3.839m and a minimum negative amplitude of -2.319m. This minimum negative amplitude or trough is 1.2m greater than FAULT A. The increased size of the trough and initial wave height has the potential to cause more damage, as there is more water going to be associated with it as well as the increased speed with which it is travelling.

The tsunami wave has the same travel pattern as the wave generated by FAULT A, which is parallel to the coast (figure 24, image 2), but it hits the coast a lot sooner, 18mins after the earthquake event.

This can be seen at the coast (figure 26), Tatapouri, Makorori and Wainui are more greatly affected. As stated previously about the FAULT A tsunami wave, this greater effect at Tatapouri can be attributed to the effects of ‘Aerial Bank’ and other rocky outcrops off the shore. The wave height at Tatapouri is still much the same height (8m) as FAULT A but it affects a much larger area and also the Wainui section of East Coast is harder hit with a 5m wave instead of the 4m wave which resulted from FAULT A and the section of coast that it is affected is a lot more pronounced.

The wave train of FAULT B seems a lot more complex than the FAULT A wave. It appears that Tuahine Point is playing a major role with the dynamics of the incoming wave; images 2 and 3 in figure 24 suggest that the bathymetry off this point gets shallower directly off Tuahine point than the surrounding area, which would explain the increased draw down and build up of water in front of the point.

The localised build up of water creates another wave that follows closely behind the initial tsunami wave and is what was responsible for the inundation (figure 25). The complex wave that is occurring seems to dampen out the effect of resonance within the bay and a random larger wave doesn't occur, as seen with the tsunami wave from FAULT A.

Chapter Six –Results

Some of what can be seen in the images from both figures 21 and 24 is the process of ‘tsunami scatter’. The lack of major structures focusing waves tends to diffuse the wave trains. This behaviour has been observed before for the March 1947 Tsunami (Downes *et al* 2000: Magill, 2001).

Mofield *et al* 2004 stated that the depth of water over topographic features is critically important to the scattering process in which shallow features are much more effective at scattering tsunami waves, while deep ones have little effect. This could explain some of the lack of intensity that is seen inside Poverty Bay compared to the coast. Aerial Bank may be assisting to scatter tsunami energy. Its location relative to the shore (15km), doesn’t help much for the exposed coast that gets most of the initial force, but it may be helping to scatter some of the wave energy before it gets into Poverty Bay.

The total distance of city inundation is 575m along the beach; less than model A despite the Lager initial wave height. It stretches from the start of Centennial Marine Drive to Churchill Park on Centennial Marine Drive (Figure 25, right). The inundation reaches 125m inland from the sand dunes; this is the northern most extent of the red on (Figure 25, right). This incorporates the main section of housing along Waikanae beach.

Chapter Six –Results

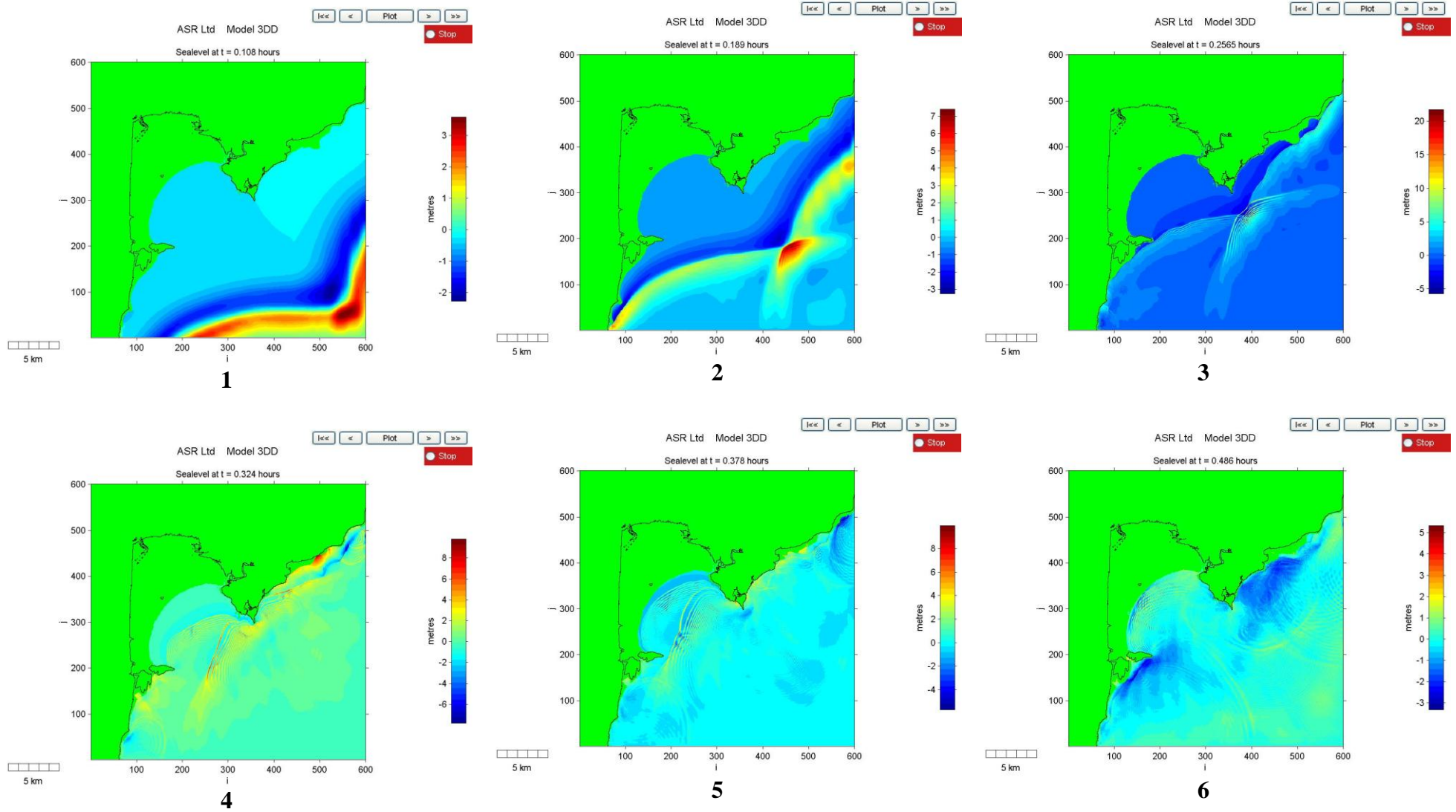
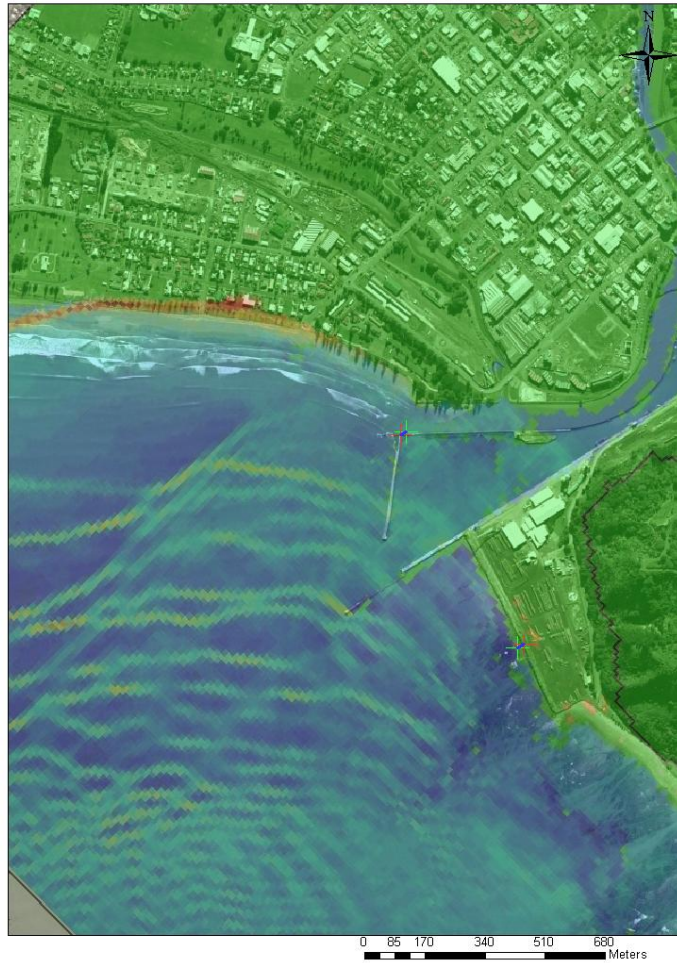


Figure 24 FAULT B Image Sequence of a Tsunami wave hitting the East Cape and Poverty Bay

**Fault B - City Inundation Map
(35mins After Earthquake)**



**Fault B - City Inundation Map
(36mins After Earthquake)**

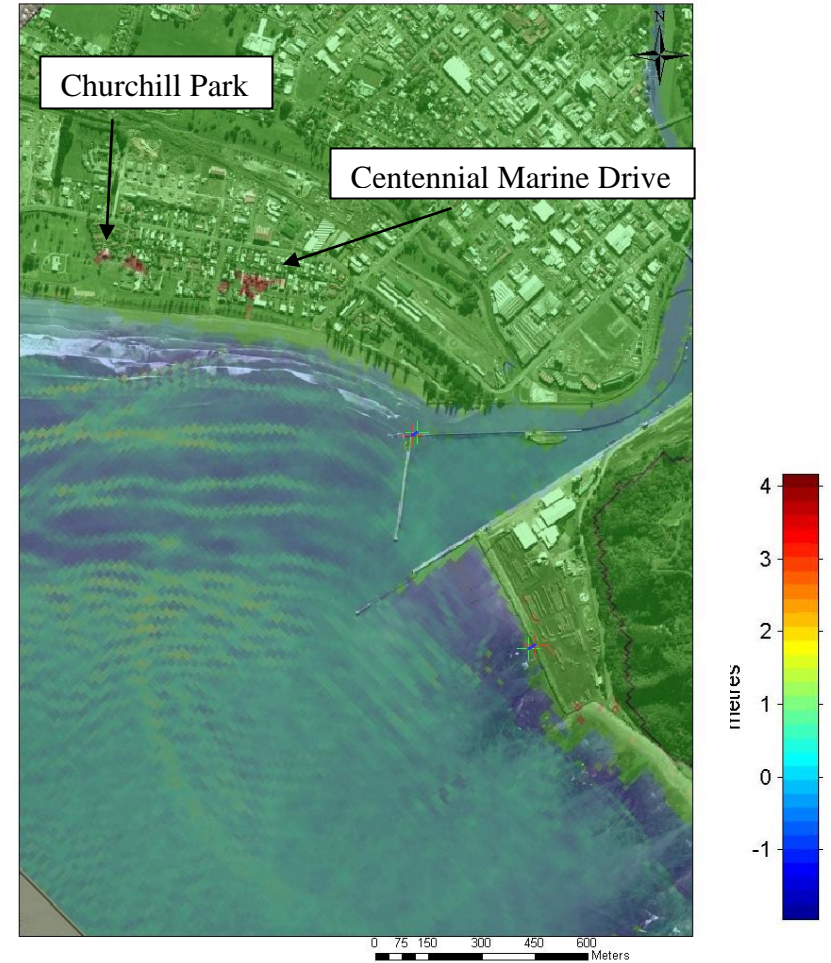


Figure 25 Inundation maps for the city from FAULT B, left shows the wave as it hits and right shows the full extent of inundation for FAULT B (Both images are overlayn on Terralink International 2005 Ltd satellite images)

Inundation Street Map of Gisborne

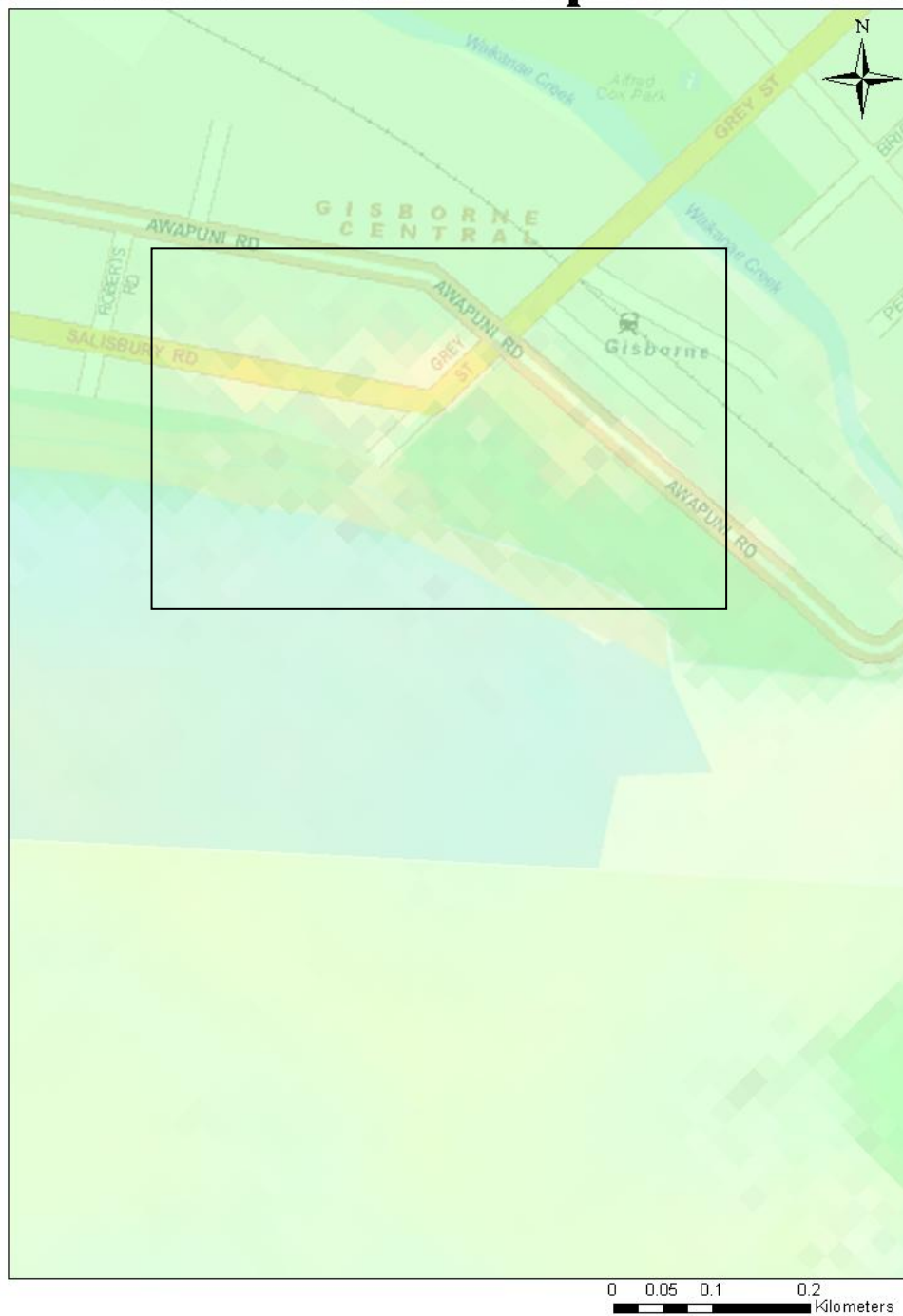


Figure 27 Inundation street map of Gisborne. Lighter coloured pixels in boxed area indicates inundation. (Terralink 2006 Street map Image)

6.3 Tsunami Bore

The transition process from tsunami bore to run-up is described by the ‘momentum exchange’ process between the bore and the small wedge-shaped water body along the shore: the bore front itself does not reach the shoreline directly, but the large bore mass pushes the initially quiescent water in front of it (Yeh 1991).

The possibility of a tsunami bore up the local rivers is a very real threat. Tsunami bores have caused substantial damage in coastal areas (Yeh 1991). This can be seen from figure 27; water is injected into the rivers once the wave has hit and it is channelled up the Turanganui, Waimata and Taruheru rivers (Figure 28). In the tsunami generated from FAULT A the bore up the rivers is about 1 – 1.5m in height; however the resulting bore height from FAULT B ranges from 2 – 2.5m.

The red circle on figure 28 (right) corresponds to figure 29, indicating the location of two of Gisborne’s emergency services (St Johns and the Fire Service) within very close proximity to the Taruheru river. A 2.5m bore would be sufficient to cause inundation and damage to these services. The white circles indicate the location of the city’s main bridges which could be severely damaged and thus cut off half the town and the worst affected coastal area from emergency services.

The tsunami bore results are only theoretical, due to the lack of any bathymetric data for the rivers. Therefore, only conservative estimates of depths were used so the final model results should not be used as a definite benchmark of what may occur in such an event.

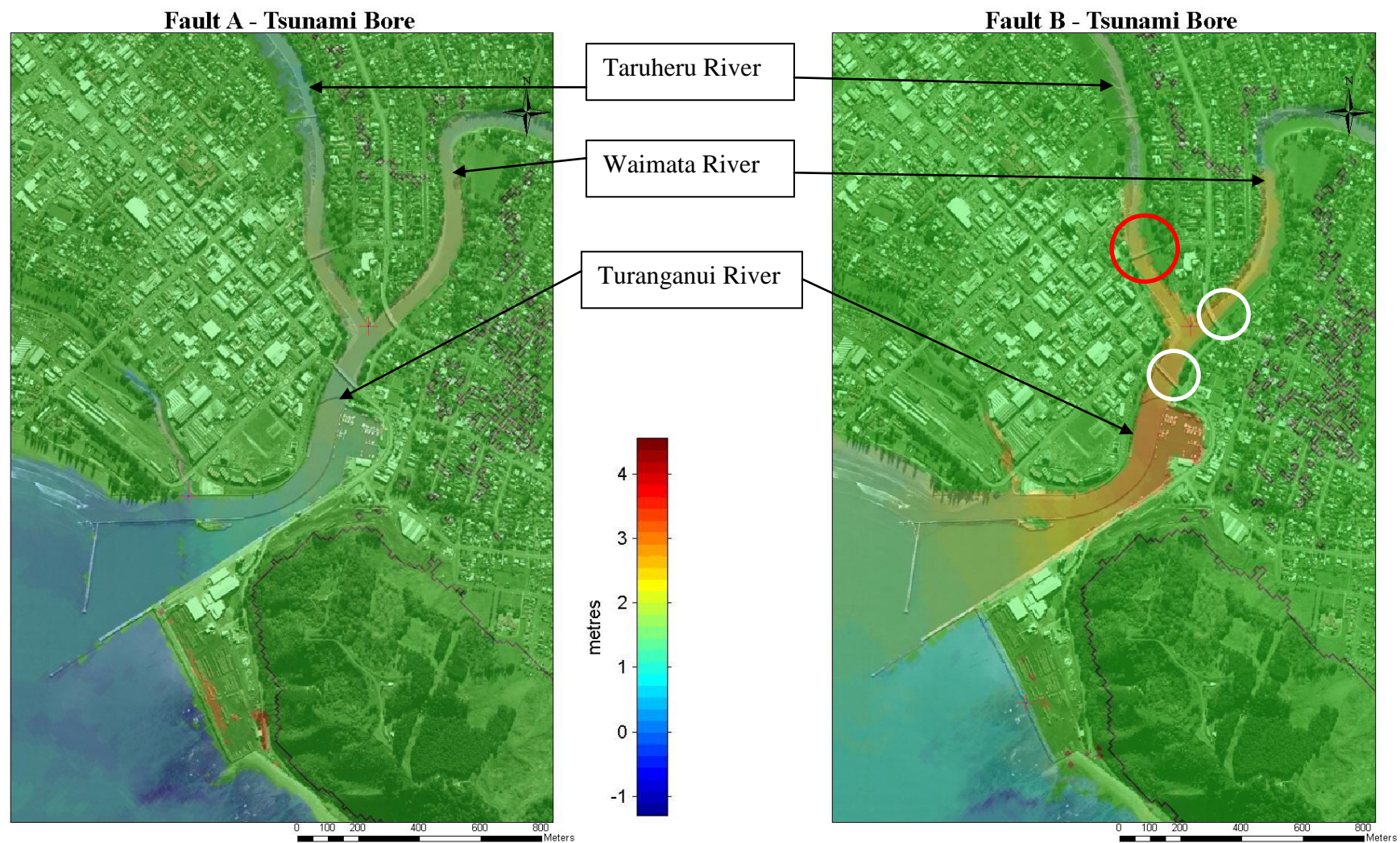


Figure 28 Tsunami bores up the rivers of Gisborne (Both images are overlayn on Terralink International 2005 Ltd satellite images)

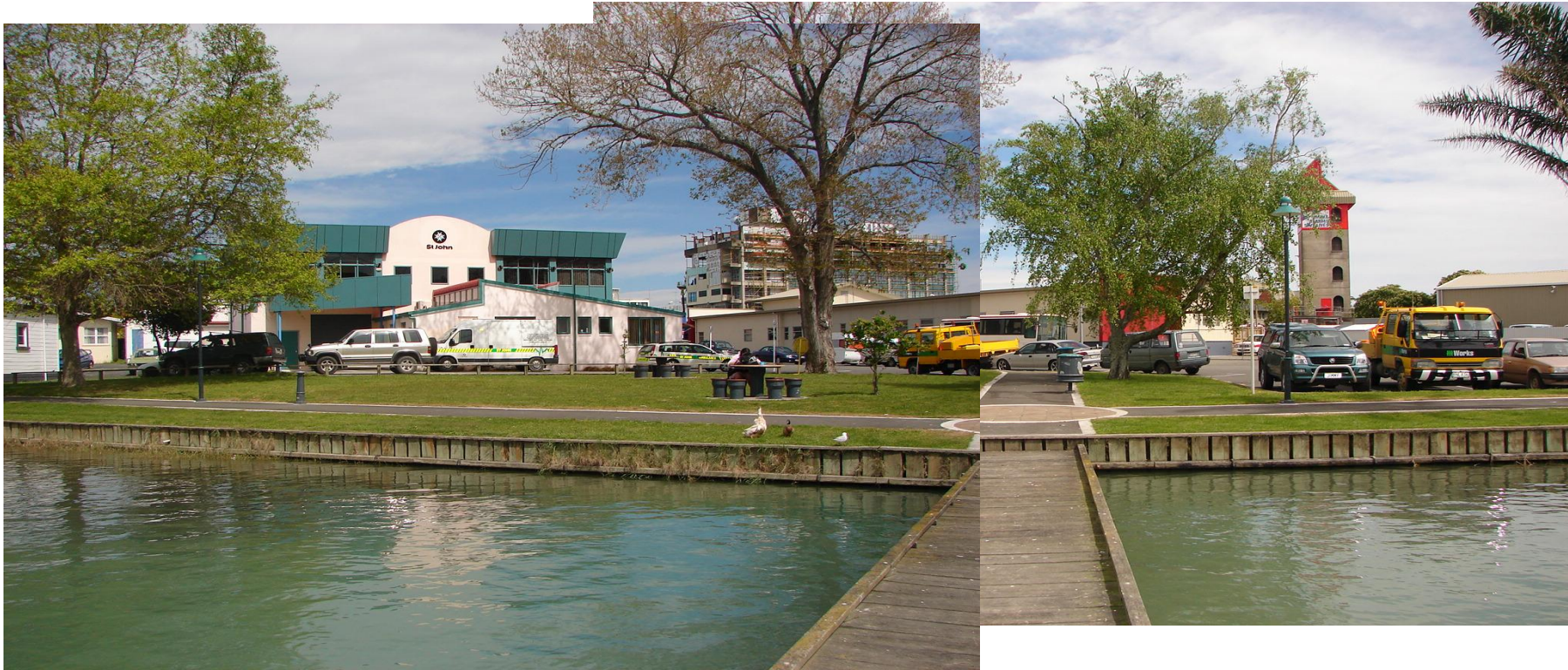


Figure 29 Corresponding to the RED circle in figure 28, Gisborne Emergency Services located on Taruheru River

CHAPTER 7 - Conclusions

7.0 Introduction

As the population of coastal areas increases the need for, and value of, scientific understanding of earthquake and tsunami hazards also increases (Mofield *et al* 2004). This is especially true, not only for Gisborne but for New Zealand. Development in Poverty Bay region along the Wainui coastline is fast growing and it is becoming a very popular place to live. With this higher density of people comes the higher risk should a tsunami event strike.

7.1 Conclusions

Numerical models were applied to consider the possible effects of an offshore earthquake generating a tsunami. The results (chapter 6) show there to be inundation from both earthquake fault scenarios modelled. The main difference in the modelled dislocations is the ‘dip’ of the fault. FAULT A has a steeper dip angle of (-25°) compared to that of FAULT B which has a dip angle of (-10°).

FAULT A had the greatest dislocation angle (-25°). Because it is a reverse fault the high positive amplitude wave (4.382m) is directed away from the coast and out to sea, this leaves the negative amplitude or wave trough propagating towards the coast and with FAULT B, it has the largest trough (-2.319m) compared to FAULT A of (-1.169m). So the angle of the dip of the dislocation plays a significant role in the size of the negative amplitude wave that is sent out towards Gisborne.

FAULT A shows an 8m wave hitting the open coast at Wainui, Makorori and Tatapouri with Tatapouri getting the hit with most of the eight meters. Most of the open coast is quite well protected with high dunes approx 5m above MSL.

Chapter Seven – Conclusions

Around Tuahine Point and into Poverty Bay the largest initial tsunami wave to hit the town beaches was 2m. This seems relatively small and insignificant since the 3m high dunes that run along the town beach would be a sufficient barrier in protecting most if not all of the residential area from the wave. However, as seen in the results 95mins after the initial earthquake event a 5m wave hits the town beach and causes substantial inundation. This wave is due to the resonant nature of the bay causing the initial waves to interact with late waves and increase their size.

The area of inundation is consistent with the distribution of sand dunes that front the beach. They average 3-4m in height (data extracted from LiDAR data) with highest at Midway Beach and decreases along the beach towards the surf club and Waikanae Cut. So inundation reaches further inland the closer you get to the residential area.

FAULT B generated tsunami has very different characteristics to its predecessor FAULT A. It has a higher initial wave which causes the wave train to scatter more and create a secondary wave due to water building up in front of Tuahine Point.

The first wave that hits the coast reacts in much the same way as the FAULT A wave in that it hits Tatapouri the hardest with an 8m wave again. However, Wainui is hit a lot harder with an initial 5m wave which is 1m higher than FAULT A. The first wave to hit the town beach is also higher with it being approximately 3m higher at 5 – 6m high. However, it doesn't cover the same area as the inundation from FAULT A even though the wave is higher. This is due to strong focusing of the wave energy, which produces the larger wave but affects a very specific area.

Chapter Seven – Conclusions

The beach fronts aren't the only area of concern when looking at tsunami inundation. Tsunami bores up rivers can cause immense damage, this is especially so in Gisborne with three rivers dividing the town along with the construction of new high rise apartments that are lining the Turanganui river bank. The FAULT B model predicts a 2.5m rise in water level, causing potential problems to the lower levels of the buildings.

As with most coastal protection measures hard structures aren't looked favourably upon, so the best measures to limit the amount of tsunami inundation and potential effects is to protect, plant and build up the natural sand dunes that already occur. This acts as a natural seawall and as seen in the first model is sufficient at keeping out an initial tsunami wave of 2m.

Planting trees is also a good natural defence mechanism, staggered planting of the exotic Norfolk Pine tree helps dissipate wave energy and decrease wave run up. This should be the main objective in protecting the emergency services along the Taruheru river.

One of the best forms of defence however is that of education combined with natural 'soft' barriers i.e. higher sand dunes and increased trees. People should be educated with the right information for what to do in the case of a tsunami. If an earthquake is felt or the sea is seen to be receding abnormally far, move inland and to higher ground.

In all the model scenarios the initial water level was taken at mean sea level not high or low tides. These factors could greatly increase or decrease the amount of inundation and destruction that is seen from a tsunami. Also in each of the model runs the East Coast is hit first and in most cases the same wave doesn't reach the town beaches until after 10 minutes later. This gives the opportunity for a base warning system to be set up on the exposed coast that would be triggered only after sufficient inundation was detected, giving the beach front residents in town a chance at evacuating to safer ground.

Chapter Seven – Conclusions

A warning system such as this could eliminate a lot of expense as it is easily maintained due to being on land and also false alarms from naturally occurring long period (which can be confused as tsunami waves) wouldn't be taken into account. It also greatly increases the towns warning system which is currently non-existent and after the recent (December 20 2007) earthquake has 85% of the local people saying they feel some form of warning system is needed (The Gisborne Herald 2008).

In 2008 it will have been 61 years since the 1947 tsunami event, and according to Fraser (1998) the return period for a 3m wave in the Gisborne harbour is 77years. Therefore, it may not be long before a wave similar to that seen from FAULT A occurs. It is also note worthy that according to the results a tsunami event of 2m saw the most inundation.

The possibility of a tsunami was very real from the December 2007 earthquake, had it been shallower it could well have been tsunamigenic.

7.2 Limitations of Research

Several limitations and difficulties were experienced when this research was carried out:

- Lack of accurate bathymetry for the bay and none for the rivers
- The labour intensive process of digitising charts
- Getting LiDAR data into a manageable size (down from 22million points)
- Insufficient bathymetry data causing unrealistic model results
- Model errors causing the models to crash, which required model grids to be rotated, have boundaries manipulated and changed, hand made boundary files, grids re-made and cropped, new origin points calculated
- Computer Model file limits of 3Gb limited some model files
- Model run times are long and delay work continuing

7.3 Further Research

Additional research could be undertaken:

- Modelling different initial condition locations to see how much earthquake location effects wave heights and travel times.
- Run model grids down to 5m for the city to get more accurate information about inundation.
- Compare model results with another tsunami modelling programme to validate models.
- Assessing the feasibility of an onshore warning system for Poverty Bay

REFERENCES

Arnadóttir T., Thornley S., Pollitz F.F. & Darby D., 1999. Spatial and temporal strain rate variations at the northern Hikurangi margin, New Zealand, *Journal of Geophysical Research.*, 104, 4931–4944.

Ayre R S, Mileti D S, Trainer P B. 1975. Earthquake and tsunami hazards in the United States : a research assessment

Berryman K. 2005. Review of Tsunami Hazard and Risk in New Zealand. Institute of Geological and Nuclear sciences clinical report 2005/104

Black K.P. 1983. Sediment transport and Tidal Inlet Hydraulics. D.Phil. Thesis, University of Waikato

Black K P. 1995. The Hydrodynamic Model 3DD and Support Software. Department of Earth Sciences, University of Waikato, Hamilton

Carter, L Foster, G. 1997. Mud sedimentation on the continental shelf at an accretionary margin - Poverty Bay, New Zealand. *New Zealand Journal of Geology and Geophysics*, 1997, Vol. 40: 157—173

Chague-Goff, Goff C J R. 2001. Catastrophic events in New Zealand Coastal Environments. GeoEnvironmental Consultants

Collot, J.-Y. J Delteil, KB Lewis, B Davy, G Lamarche. 1996. From oblique subduction to intra-continental transpression: structure of the southern Kermadec–Hikurangi margin from multibeam bathymetry, side-scan sonar and seismic reflection, *Marine Geophysical. Research.*, 18, 357–181.

References

Dengler L. 1998. Strategic Implementation Plan for Tsunami Mitigation Projects. NOAA Technical Memorandum ERL PMEL-113, Department of Geology Humboldt State University.

de Lange W.P. and Healy T.R. 1986. New Zealand Tsunamis 1840 – 1982. *New Zealand Journal of Geology and Geophysics* 29(1), 115-134

de Lange W.P. 1998. Tsunami Generation by Diapiric Piercement (Mud Volcanism). AGU 1998 Fall Meeting.

de Lange W.P. and Fraser R. 1999. Overview of Tsunami Hazard in New Zealand. *Tephra* 18: 3-9

de Lange W.P., Healy T. 1999. Tsunami and tsunami hazard. *Tephra* 18: 13-20

de Lange W.P. and Healy, T.R. 1997: Numerical modelling of tsunamis associated with marl diapirism off Poverty Bay, New Zealand. In *Pacific Coasts and Ports '97: Proceedings of the 13th Australasian Coastal and Ocean Engineering Conference and 6th Australasian Port and Harbour Conference*, Christchurch: Centre for Advanced Engineering, University of Canterbury, 1043–47.

Doser I. D and Webb T. H. 2003. Source parameters of large historical (1917–1961) earthquakes, North Island, New Zealand. *Geophysical Journal International* 152 (3), 795–832

Downes G.L., Webb T., McSaveney M., Darby D., Doser D., Cagué-Goff C., Barnett A. 2000. The March 25 and May 17, 1947 Gisborne earthquakes and tsunami: implications for tsunami hazard for east coast, North Island, New Zealand, *Proc. Tsunami Risk Assessment Beyond 2000: Theory, Practice and Planning*, Moscow, 55-67

Eiby G.A. 1982. Two New Zealand tsunamis. *Journal of the Royal Society of New Zealand* 12: 337-351.

References

Figure 1 retrieved from, www.surforecast.com/locationmaps/TolagaBay.jpg

Figure 4 retrieved from, www.andaman.org/mapstsunami/3tsunami/3tsunami.htm

Fraser R.J. 1998. Historical Tsunami Database for New Zealand. M.Sc Thesis, Department of Earth Sciences, The University of Waikato.

Grapes R., Downes, G. 1997. The 1855 Wairarapa, New Zealand, earthquake - analysis of historical data, *Bulletin of the New Zealand Society for Earthquake Engineering* 30: 271-369.

Healy T., Stephens S., Black-K., Gorman R., Cole R., Beamsley B. 2002. Port redesign and planned beach renourishment in a high wave energy sandy-muddy coastal environment, Port Gisborne, New Zealand. *Geomorphology* 48(1-3)

Heath R.A. 1985. A review of the physical oceanography of the seas around New Zealand — 1982. New Zealand Oceanographic Institute Division of Marine and Freshwater Science

Heath R. A. 1982. Generation of 2-3-hour oscillations on the east coast of New Zealand. *New Zealand Journal of Marine and Freshwater Research*, 1982. 16: 111-117

Hull,A.G. 1986. Pre-A.D. 1931 tectonic subsidence of Ahuriri Lagoon, Napier, Hawke's Bay, New Zealand *New Zealand Journal of Geology and Geophysics* 29: 75-82.

Jones J. 2008. Mayor sees no need to add to CD alert plans. *The Gisborne Herald*. Tuesday 8th of January 2008.

Karling H. M., 2005. *Tsunamis: The Great Wave*. Nova Science Publishers, Inc. New York.

Kienle J., Kowalik Z., Murty T.S. 1987. Tsunamis Generated by Eruptions from Mount St. Augustine Volcano, Alaska. *Science* 236, 1442-1447.

References

Lander J F, Lockridge P A, Whiteside L S. 2003. TWO DECADES OF GLOBAL TSUNAMIS - 1982-2002. The International Journal of The Tsunami Society. 21(1).

Lewis B.K., Collot J., Lallemand S. E. 1998. The dammed Hikurangi Trough: a channel-fed trench blocked by subducting seamounts and their wake avalanches (New Zealand –France GeodyNZ Project). Basin research 10, 441-468

Lewis B.K., Collot JY., Goring D. 1999. Huge Submarine Avalanches: is there a risk of giant waves and, if so where? Tephra 18: 21-29

Liu, P. L.-F., Synolakis, C. E., and Yeh, H., 1991. Impressions from the First International Workshop on Long Wave Runup, Journal of Fluid Mechanics, 229, 675 688.

Lockridge P.A. 1990. Nonseismic phenomena in the generation and augmentation of tsunamis. Natural Hazards. 3(4): 403-412

Magill C.R. 2001. Numerical Modelling of Tsunami Generated by Mass Movement M.Sc. Thesis, Department of Earth Sciences, The University of Waikato.

Mansinha L., Smylie D.E. 1971. The Displacement Fields of Inclined Faults. Bulletin of the Seismological Society of America. Vol 61, No 5. 1433-1440.

McGinty P., Reyners M., Robinson R. 2000. Stress directions in the shallow part of the Hikurangi subduction zone, New Zealand , from the inversion of earthquake first motions. Geophysics Journal International 142, 339-350

McGuire W.J. 1996. Volcano instability: a review of contemporary themes. In volcano Instability on Earth and Other Planets, edited by W.J. McGuire, A.P. Jones and J. Neuberg. Geological Society Special Publication No. 110. The Geological Society, Bath, UK

References

Mofield H.O., Symons C.M., Lonsdale P., Gonzalez F.I., Titov V.V. 2004. Tsunami Scattering and Earthquake Faults in the Deep Pacific Ocean. *Oceanography – Special Edition*, Vol 17 No. 1

Moore J.G., Clague D.A., Holcomb R.T., Lipman P.W., Normark W.R., Torresan M.E. 1989. Prodigious Submarine Landslides in the Hawaiian Ridge. *Journal of Geophysical Research* 94(B12), 17465-17484

Morgan J. 1984. Science of Tsunami Hazards, *The International Journal of The Tsunami Society*. 2(1)

Parnell K., Shepherd M.J., Hesp P.A.(1999). Coastal geomorphology in New Zealand, 1989–99. *Progress in Physical Geography* 23, 501–524

Pishief K.S. 2006. Community Understanding and Preparedness for Tsunami Risk in the Eastern North Island, New Zealand. Masters of Science Thesis. University of Waikato

Rayners M. 1998. Plate coupling and the hazard of large subduction thrust earthquakes at the Hikurangi subduction zone, New Zealand, *Journal of Geology and Geophysics* 41, 343-354

Rayners M., McGinty P. 1999. Shallow subduction tectonics in the Raukumara Peninsula, New Zealand, as illuminated by earthquake focal mechanisms. *Journal of Geophysical Research*. 104, No B2 3025-3034

Siebert L., Begét J.E., Glicken H. 1995. The 1883 and Late-Prehistoric Eruptions of Augustine Volcano, Alaska. *Journal of Volcanology and Geothermal Research* 66, 367-395 (used?)

Stevenson D. 2005. Tsunamis and Earthquakes: What Physics is Interesting? *Physics Today*, American Institute of Physics. 10-11

References

Tinti S., Bortolucci E., Armigliato A. 1999a. Numerical simulation of the landslide-Induced tsunami of 1988 on Vulcano, Italy. *Physics and Chemistry of the Earth* 24(5), 423-429

Tinti S., Bortolucci E., Romagnoli C. 2000. Computer simulations of tsunamis due to sector collapse at Stromboli, Italy. *Journal of Volcanology and Geothermal Research* 96, 103-128

Ward S.N., Day S. 2001. Suboceanic Landslides. For Publication in: 2002 *Yearbook of Science and Technology McGraw-Hill*. 1.2

Webb T.H., Wesnousky, S.G., Helmberger D.V. 1985. A body-wave analysis of the 1966 Gisborne, New Zealand, earthquake. *Tectonophysics*, 133, 271-282

Webb T.H., Anderson H. 1998. Focal mechanisms of large earthquakes in the North Island of New Zealand: Strain partitioning at an oblique active margin, *Geophys. J. Int.*, 134, 40-86

Whyte, 1984 P. Whyte , *Gisborne's Battle for a Harbour.*, Gisborne Harbour Board, Gisborne (1984) p152.

Wright I. C., Gamble J A., Shane P. A. 2003. Submarine, silicic volcanism of the Healy caldera, southern Kermadec arc (SW Pacific): I – volcanology and eruption mechanisms. *Bulletin of Volcanology* 65, 15-29

Velichko A.S., Dotsenko S.F., Potetyunko É.N. 2002. Amplitude-Energy Characteristics of Tsunami Waves for Various types of Seismic Sources Generating Them. *Physical Oceanography*, Vol. 12, No. 6

Yeh H.H. 1991. Tsunami Bore Runup. *Natural Hazards*. vol. 4. 209-220